Kumari Priti PALLAVI

Priti thesis final

Conference Paper

Document Details

Submission ID
trn:oid:::27535:141052279

Submission Date
May 30, 2026, 8:16 PM GMT+5:30

Download Date
May 30, 2026, 8:26 PM GMT+5:30

File Name
Priti thesis final.pdf

File Size
1.1 MB

69 Pages

17,204 Words

103,620 Characters

9% Overall Similarity

The combined total of all matches, including overlapping sources, for each database.

Filtered from the Report

- Bibliography
- Quoted Text
- Cited Text
- Small Matches (less than 10 words)

Match Groups

130 Not Cited or Quoted 9%
Matches with neither in-text citation nor quotation marks

0 Missing Quotations 0%
Matches that are still very similar to source material

0 Missing Citation 0%
Matches that have quotation marks, but no in-text citation

0 Cited and Quoted 0%
Matches with in-text citation present, but no quotation marks

Top Sources

4% Internet sources
5% Publications
7% Submitted works (Student Papers)

Integrity Flags

0 Integrity Flags for Review

Our system's algorithms look deeply at a document for any inconsistencies that would set it apart from a normal submission. If we notice something strange, we flag it for you to review.

A Flag is not necessarily an indicator of a problem. However, we'd recommend you focus your attention there for further review.

Match Groups

- **130** Not Cited or Quoted 9%
  Matches with neither in-text citation nor quotation marks
- **0** Missing Quotations 0%
  Matches that are still very similar to source material
- **0** Missing Citation 0%
  Matches that have quotation marks, but no in-text citation
- **0** Cited and Quoted 0%
  Matches with in-text citation present, but no quotation marks

Top Sources

- 4% Internet sources
- 5% Publications
- 7% Submitted works (Student Papers)

Top Sources

The sources with the highest number of matches within the submission. Overlapping sources will not be displayed.

1	Student papers	
University of Hertfordshire on 2026-03-27		<1%
2	Internet	
dokumen.pub		<1%
3	Student papers	
I. K. Gujral Punjab Technical University on 2026-04-06		<1%
4	Internet	
ies.ieee-ies.org		<1%
5	Internet	
gyan.iitg.ac.in		<1%
6	Student papers	
University of Central Lancashire on 2025-05-18		<1%
7	Student papers	
Jawaharlal Nehru Technological University on 2024-12-21		<1%
8	Internet	
umpir.ump.edu.my		<1%
9	Publication	
Anurag Tiwari. "Power quality enhancement in grid-connected PV systems with b...		<1%
10	Student papers	
Liverpool John Moores University on 2024-05-26		<1%

11 Publication
Vigneysh, T., and N. Kumarappan. "Autonomous operation and control of photov... <1%

12 Publication
Zhining Zhang, Boxue Hu, Yue Zhang, Pengyu Fu, Jin Wang, Jacob Mueller, Lucian... <1%

13 Student papers
IIT Delhi on 2014-07-26 <1%

14 Internet
publikationen.bibliothek.kit.edu <1%

15 Student papers
University of Strathclyde on 2026-04-02 <1%

16 Student papers
Jawaharlal Nehru Technological University on 2011-07-11 <1%

17 Student papers
Uttar Pradesh Technical University on 2024-10-17 <1%

18 Student papers
Anna University on 2026-05-07 <1%

19 Publication
Xiaoyu Wang, Meng Yue, Eduard Muljadi. "Modeling and control system design fo... <1%

20 Student papers
University of Teesside on 2025-01-05 <1%

21 Student papers
IIT Delhi on 2017-03-16 <1%

22 Internet
icsgistanbul.com <1%

23 Publication
Francisco Rodrigues Lima, Lauro Osiro, Luiz Cesar R. Carpinetti. "A fuzzy inferenc... <1%

24 Student papers
Heriot-Watt University on 2018-08-29 <1%

25 Student papers
IIT Delhi on 2017-02-17 <1%

26 Student papers
University of Nottingham on 2026-05-07 <1%

27 Internet
ir.kluniversity.in <1%

28 Internet
www.frontiersin.org <1%

29 Student papers
Engineering Institute of Technology on 2024-12-01 <1%

30 Student papers
University Of Tasmania on 2011-10-18 <1%

31 Student papers
University of Teesside on 2023-05-08 <1%

32 Internet
assets-eu.researchsquare.com <1%

33 Internet
deepblue.lib.umich.edu <1%

34 Student papers
IIT Delhi on 2015-11-07 <1%

35 Student papers
RMIT University on 2021-05-30 <1%

36 Publication
Shadab Murshid, Bhim Singh. "Implementation of PMSM Drive for a Solar Water P... <1%

37 Student papers
University of Liverpool on 2013-09-09 <1%

38 Internet
prism.ucalgary.ca <1%

39 Internet
res.mdpi.com <1%

40 Internet
uu.diva-portal.org <1%

41 Internet
www.researchgate.net <1%

42 Student papers
College of the North Atlantic-Qatar on 2026-05-12 <1%

43 Student papers
IIT Delhi on 2014-09-12 <1%

44 Publication
P.R. Souza, G.L. Dotto, N.P.G. Salau. "Artificial neural network (ANN) and adaptive ... <1%

45 Student papers
University of Sheffield on 2015-12-11 <1%

46 Internet
discovery.researcher.life <1%

47 Internet
kupdf.net <1%

48 Internet
www.acarindex.com <1%

49 Internet
www.neexgent.com <1%

50 Internet
www.slideshare.net <1%

51 Publication
"A New Method for Determining Reference Compensating Currents of Three-Pha... <1%

52 Publication
Bhim Singh. "Power Balance Theory Based Control of an Electronic Load Controlle... <1%

53 Publication
Dong-Choon Lee. "Unified active power filters for source voltage unbalance/curre... <1%

54 Student papers
Edith Cowan University on 2026-05-26 <1%

55 Publication
Gajjar, Nimita Ashish. "A Novel Control of Grid Tied PV- DSTATCOM System.", Guja... <1%

56 Student papers
Harcourt Butler Technical University on 2026-05-15 <1%

57 Publication
I. Serban, C. Marinescu. "A look at the role and main topologies of battery energy ... <1%

58 Student papers
IIT Delhi on 2014-12-31 <1%

59 Publication
K. V. Sambasivarao, Anasuya Sesha Roopa Devi Bhima. "Artificial Intelligence, Co... <1%

60 Student papers
National Institute of Technology, Rourkela on 2014-05-09 <1%

61 Publication
Remya K., Sasi K. Kottayil. "Active Power Control in Variable Speed Wind Electric G... <1%

62 Student papers
University of Edinburgh on 2014-08-18 <1%

63 Student papers
University of Nottingham on 2019-07-28 <1%

64 Student papers
University of Nottingham on 2021-09-10 <1%

65 Student papers
University of Wales Swansea on 2024-05-01 <1%

66 Student papers
Victoria University on 2017-11-15 <1%

67 Publication
Y.H.A. Rahim, A.L. Mohamadien, A.S. Al Khalaf. "Comparison between the steady-... <1%

68 Internet
academic-accelerator.com <1%

69 Internet
irjet.net <1%

70 Internet
uiassist.org <1%

71 Internet
www.hindawi.com <1%

72 Publication
"Renewable Power for Sustainable Growth", Springer Science and Business Media... <1%

73 Student papers
Bahrain Polytechnic on 2025-05-19 <1%

74 Student papers
City University on 2017-09-11 <1%

75 Publication
Dao Zhou, Yipeng Song, Frede Blaabjerg. "Modeling and Control of Three-Phase A... <1%

76 Publication
Debatosh Guha, Badal Chakraborty, Himadri Sekhar Dutta. "Computer, Communi... <1%

77 Student papers
Glasgow Caledonian University on 2018-05-25 <1%

78 Publication
Gonzalez-Espin, Fran, Gabriel Garcera, Ivan Patrao, and Emilio Figueres. "An Adap... <1%

79 Publication
H. Scheer, B. McNelis, W. Palz, H.A. Ossenbrink, P. Helm. "Sixteenth European Pho... <1%

80 Student papers
IIT Delhi on 2015-05-04 <1%

81 Student papers
IIT Delhi on 2015-06-29 <1%

82 Student papers
IIT Delhi on 2017-01-12 <1%

83 Student papers
IIT Delhi on 2017-03-28 <1%

84 Publication
M. H. Haque. "Characteristics of shunt, short-shunt and long-shunt single-phase i... <1%

85 Publication
Mrutyunjaya Mangaraj, Trilochan Penthia, Anup Kumar Panda. "Implementation ... <1%

86 Publication
Navaneethakkannan, C., and M. Sudha. "Analysis and Implementation of ANFIS-b... <1%

87 Publication
Nirav Patel, Nitin Gupta, Ramesh C. Bansal. "Combined active power sharing and ... <1%

88 Publication
S.R. Reddy, P.V. Prasad, G.N. Srinivas. "Design of PI and Fuzzy Logic Controllers fo... <1%

89 Publication
Sara Mahmoudi Rashid, Amir Rikhtehgar Ghiasi. "Energy management enhancem... <1%

90 Student papers
Sheffield Hallam University on 2025-01-06 <1%

91 Publication
Sombir Kundu, Madhusudan Singh, Ashutosh K. Giri. "Adaptive Control Approach-... <1%

92 Student papers
Texas A & M University, Kingville on 2023-04-16 <1%

93 Publication
Ujwala Gajula, Gouthami Eragamreddy, N. Malla Reddy, Remala Geshma Kumari, ... <1%

94 Publication
Ulrich Tietze, Christoph Schenk. "Advanced Electronic Circuits", Springer Nature, ... <1%

95 Student papers
Universite De Tlemcen on 2026-03-18 <1%

96 Student papers
University of Greenwich on 2020-04-24 <1%

97 Student papers
University of Hertfordshire on 2026-03-27 <1%

98 Student papers
Uttar Pradesh Technical University on 2026-04-29 <1%

99 Internet
aece.ro <1%

100 Internet
engrxiv.org <1%

101 Internet
id.scribd.com <1%

102 Internet
mafiadoc.com <1%

103 Internet
ndl.ethernet.edu.et <1%

104 Internet
upcommons.upc.edu <1%

105 Internet
www.scirp.org <1%

CHAPTER 1

INTRODUCTION

1.1 Introduction to Renewable Energy and Hybrid Microgrid Systems

The world is in a stage of transition from traditional energy facility generation to decentralised renewable energy systems (RES) due to two key considerations: energy security and environmental sustainability. By combining several energy sources like solar photovoltaics (PV) and wind energy, Hybrid Renewable Energy Systems (HRES) provide a strong alternative to solving the intermittency of single renewable energy sources. Isolated hybrid microgrids provide the main supply of electricity to locations where the costs of connecting to the electricity grid are too high. These microgrids are small power units that can work independently of the main power grid, which makes them difficult to manage so that they can balance the generation of power and demand for it. In these standalone systems, the key problem is that there is no necessarily stiff grid to give inertia to the system, and they are therefore sensitive to changes in environmental conditions and to load disturbances.

1.2 Solar PV, Wind Energy Conversion System, and Self-Excited Induction Generator (SEIG)

The proposed isolated micro-grid is a combination of a solar PV system and a Wind Energy Conversion System (WECS) as the main energy sources. The solar PV system is based on the principle of photoelectric effect and directly converts the solar irradiance into DC power using the PV system and then the DC power is conditioned by boost converter. To complement this, the WECS converts the wind kinetic energy into electricity via a wind turbine that is mechanically connected to a Self-Excited Induction Generator (SEIG). The SEIG is particularly designed for stand-alone applications because of its inherent advantages, which include no separate DC excitation source, strong squirrel cage structure, and low maintenance. The SEIG, however, is a highly non-linear machine whose terminals are strictly controlled by the excitation capacitance, rotor speed and the load connected to it. The SEIG must rely on a shunt capacitor bank to start the self-excitation process by means of the residual magnetism of the rotor iron, unlike synchronous generators.

1.3 Power Quality Problems in Isolated Hybrid Microgrids

Within isolated microgrids, Power quality becomes damaged because of two primary elements including the random behavior of renewable energy generating sources and the usage of non-linear loads. Severe voltage sags, swells, and frequency changes are created by inconsistent solar light and changing wind velocities, which might cause sensitive electronic hardware components to fail. Experts claim that the increasing amount of non-linear loads, such as bridge rectifiers and variable speed drives, brings harmonic distortions and reactive power load pressures at the point of common coupling (PCC). It has been observed that uncompensated isolated systems show source current THD amounts reaching 25.5% in various research reports, so active reduction methodologies are required to follow IEEE 1547 and IEEE 519 standards. Voltage instability grows worse when the reactive power needs of the SEIG and the linked inductive loads increase, which can cause a total voltage system failure when heavy loading or motor starting activities happen.

1.4 Role of DSTATCOM and Battery Energy Storage System (BESS)

To overcome the above PQ problems a Distribution Static Synchronous Compensator (DSTATCOM) is integrated at the PCC. The DSTATCOM, functioning as a shunt active power filter, provides real time reactive power compensation, load balancing and harmonic mitigation. It is composed of a three phase Voltage Source Converter (VSC) that injects compensating currents into the network to cancel the harmonic components consumed by non-linear loads. A Battery Energy Storage System (BESS) is connected to the VSC dc-link to enhance the dynamic stability of the microgrid. The BESS serves as an energy buffer to absorb excess power in times of high generation and to inject active power in the case of generation shortfalls. This coordination guarantees the control of the DC-link voltage, which is critical for the proper functioning of the DSTATCOM and the overall frequency stability of the isolated system.

1.5 DTOGI-PLL Synchronization

Accurate synchronism is required to effectively control grid-connected or stand-alone VSCs. The conventional Synchronous Reference Frame Phase-Locked Loops (SRF-PLL) are usually not effective in isolated microgrids because of high harmonic pollution and unbalanced voltages. To overcome these limitations, the Dual Third-Order Generalized Integrator (DTOGI) based PLL is used in this work. The DTOGI-PLL employs a dynamic pre-filtering stage to extract the fundamental positive sequence

component of the PCC voltage even in case of severe distortion. The DTOGI-PLL improves the rejection of DC offsets and harmonic noise, ensuring the DSTATCOM is properly synchronized with the microgrid frequency; this prevents phase-offset errors and degradation of the control system performance during transient load changes.

1.6 ANFIS-Based Intelligent Control Techniques

The robustness of conventional Proportional-Integral (PI) controllers is limited due to high non-linearity and parameter uncertainties in SEIG based microgrids. Proposed work implements intelligent alternative for frequency control using Adaptive Neuro-Fuzzy Inference System (ANFIS). ANFIS combines the transparent reasoning of Fuzzy Logic Systems with the learning and adaptation capabilities of Artificial Neural Networks. The ANFIS controller can adaptively tune its membership functions and rule base using frequency error and its derivative as inputs, thus achieving a faster and more stable response than controllers with fixed gains. The ANFIS reduces the settling time and the overshoot in DC-link regulation significantly while providing high precision for BESS to compensate power imbalances.

1.7 Motivation, Research Gap, and Need for Proposed Work

The pressing necessity to supply remote standalone settlements with dependable, high-quality power is the driving force for this study. Although isolated microgrids have been studied in the literature, current approaches still have a number of drawbacks. Because of the SEIG's non-linear magnetizing properties, many systems rely on conventional PI controllers. Furthermore, weak grids with high harmonic content and low inertia frequently show instability when using typical synchronization approaches. The creation of a unified control system that simultaneously solves robust synchronization and adaptive frequency regulation in hybrid PV-Wind-SEIG designs is a major research gap. To guarantee compliance with IEEE 1547 standards under dynamic loading situations, an integrated method that combines the robust filtering of DTOGI-PLL with the learning capabilities of ANFIS is desperately needed.

1.8 Research Objectives and Scope of the Work

Hybrid PV-wind-SEIG microgrids provide a productive method for producing electricity in distant locations, yet these hybrid PV-wind-SEIG microgrids possess various technical difficulties regarding reactive power unevenness, frequency shifts,

harmonic distortion, and voltage unsteadiness. Because the Self-Excited Induction Generator contains nonlinear traits and renewable energy sources have an unstable character, the hybrid PV-wind-SEIG microgrids become very sensitive when working situations or load interferences change. Experts claim that nonlinear loads elevate the harmonic distortion of the hybrid PV-wind-SEIG microgrids by a large margin, which reduces the effectiveness of the arrangement and creates low power excellence. Traditional synchronization and management strategies fail to provide adequate active results when the hybrid PV-wind-SEIG microgrids experience distorted or uneven functional environments. The maintenance of steady frequency control and the following of IEEE-1547 harmonic requirements for the hybrid PV-wind-SEIG microgrids in separated networks are regarded as a hard task by many people. An enhanced intelligent control framework that can concurrently improve harmonic correction, synchronization precision, and system stability is therefore required.

The following are the main objective of this study:

- to create a MATLAB/Simulink hybrid PV-wind-SEIG isolated microgrid model.
- to use BESS interfaced with DSTATCOM for harmonic mitigation and reactive power support.
- to use DTOGI-PLL for precise synchronization in distorted environments.
- to create an intelligent frequency controller based on ANFIS for improved dynamic responsiveness.
- to achieve THD performance that complies with IEEE-1547 under nonlinear loading circumstances.
- to evaluate system performance in imbalanced and dynamic operating environments.

1.9 Organisation of the Thesis

Chapter 1- Introduction

This chapter presents the background of hybrid renewable energy systems and power quality issues in isolated microgrids. It also discusses the research objectives, motivations, proposed methodology and scope of the work.

Chapter 2- Literature Review

This chapter provides a review of previous studies related to SEIG, DSTATCOM, BESS, synchronisation techniques, and intelligent control methods. It also identifies the research gaps and the need for the proposed study.

Chapter 3- System configuration

This chapter describes the configuration of the proposed hybrid PV-Wind-SEIG microgrid and its associated subsystems. It also explains the DTOGI-PLL synchronisation, ANFIS controller, and overall control strategy.

Chapter 4- Result and Discussion

This chapter presents the MATLAB/Simulink implementation and performance evaluation of the proposed system. The obtained results are analysed under steady-state and dynamic operating conditions.

Chapter 5- Conclusion and Future Scope

This chapter summarises the important findings and contributions of the proposed research work. It also provides limitations of the present study and recommendations for future research direction.

CHAPTER 2

LITERATURE REVIEW

2.1 Introduction

An isolated hybrid PV-Wind-SEIG microgrid's intelligent control framework design necessitates a thorough synthesis of earlier research from a number of related technical fields. Various technical areas like SEIG modeling and regulation, DSTATCOM-based active power quality conditioning, BESS integration strategies, PLL synchronization techniques, DTOGI algorithm, ANFIS frequency control, and IEEE Standard 1547 compliance are found in this scholarly territory. Experts claim that the chapter provides a critical review of typical contributions in each specialized sector because the chapter is structured from generation fundamentals through power quality challenges to sophisticated control solutions. A combined finding of research gaps which directly drive the proposed academic effort is presented when the chapter reaches the end.

2.2 Self-Excited Induction Generator-Based Microgrids

Basic ideas of self-excitation were created through systematic nodal admittance analysis of the SEIG circuit [1]. Specialized professionals claim that stable terminal voltage build-up needs the capacitive reactive supply to be larger than machine magnetizing demand because this must happen at all operating frequencies [1]. A comprehensive survey of SEIG modelling methods including equivalent circuit analysis, d-q axis formulation, and iterative computational approaches subsequently identified dynamic reactive power compensation as the essential remediation for poor voltage regulation under variable loads, directly motivating the DSTATCOM architecture employed in the present work [2]. The practical design of low-cost SEIG systems for remote electrification was investigated to confirm cost and maintenance advantages over synchronous generators, subject to the availability of active compensation [3]. A VSC-based scheme for combined voltage and frequency control of a standalone wind-driven SEIG was presented and validated under balanced linear loads; however, harmonic distortion and unbalanced loading were not evaluated [4]. STATCOM-based voltage regulation for SEIGs under varying loads was demonstrated through simulation and experiment, though the study was restricted to balanced resistive-inductive conditions without consideration of nonlinear loading or power quality compliance [5].

2.3 DSTATCOM Applications and Power Quality Enhancement

The Synchronous Reference Frame (SRF) theory was systematized as the principal analytical framework for active power conditioner reference current generation, demonstrating that dq-frame decomposition of load current into its fundamental active component and the residual reactive-harmonic remainder enables precise DSTATCOM compensation reference computation [6]. The instantaneous p-q theory was developed as a complementary approach operating directly in the αβ stationary frame; however, its sensitivity to PCC voltage distortion a critical limitation in isolated SEIG microgrids where the source voltage is itself distorted —was identified as a fundamental constraint [7]. A comparative evaluation of VSC current control strategies established that hysteresis current control offers the optimal combination of simplicity, inherent current limiting, and dynamic response for DSTATCOM applications, making it the strategy of choice in the present work [8]. Power quality improvement using DSTATCOM supported by BESS was demonstrated under nonlinear loads, but the conventional PI-SRF control employed exhibited performance degradation under the distorted and unbalanced voltage conditions characteristic of isolated SEIG operation [9]. A model predictive control approach for a grid-integrated hybrid microgrid achieved tight DC-link voltage regulation and low THD, but was limited to grid-connected operation and did not address islanded SEIG conditions [10].

2.4 Battery Energy Storage System Integration

A three-level hierarchical control architecture for droop-controlled AC/DC microgrids with integrated energy storage established that primary droop control achieves autonomous power sharing, whilst secondary and tertiary layers provide frequency restoration and economic optimization the conceptual framework within which the PI-regulated bidirectional DC-DC converter (BDC) of the present work is situated [11]. A closely related prior work presented DTOGI-CDSC-FLL-based synchronization and control of a WEC-PV-BESS distributed generation system, demonstrating superior power quality under distorted grid conditions [12]. However, that study addressed grid-connected DG rather than islanded SEIG operation and employed an FLL rather than ANFIS for frequency control, leaving the specific challenges of isolated SEIG microgrid regulation unresolved. The shared DC-link architecture adopted in the present work wherein the BESS interfaces the DSTATCOM VSC DC bus through the

BDC achieves real power balancing and reactive-harmonic compensation within a single conversion stage, maximizing energy conversion efficiency [9], [11].

2.5 Phase-Locked Loop Synchronisation Techniques

A comprehensive review of the SRF-PLL documented its well-known degradation under unbalanced conditions, wherein negative-sequence voltage components produce double-frequency oscillations in the dq-frame that contaminate phase angle estimates and DSTATCOM reference currents [7]. A PLL structure based on the second-order generalized integrator (SOGI-PLL) was proposed, in which an adaptive bandpass filter at the fundamental frequency pre-processes the measured voltage prior to locking, substantially improving harmonic rejection; however, the second-order roll-off limits attenuation of low-order harmonics and DC offset [8]. Many people believe that standard PLL structures are weak when supply conditions vary and have distortion [9]. A necessary requirement for strong pre-filtering was shown for synchronization in distributed generation working applications because strong pre-filtering provides reliability [9]. MFLL showed very good performance outcomes when distortion is bad because MFLL uses many resonant filters for harmonic orders [10]. Computational complexity and parameter sensitivity increase when MFLL is used, even though MFLL works well under distortion [10]. Researchers have observed that DTOGI-PLL is better than all SOGI-based options for harmonic rejection and DC offset immunity [11]. DTOGI-PLL uses a third-order integrator structure while the implementation complexity stays in the middle [11]. Because DTOGI-PLL has these features, DTOGI-PLL is the best selection for the distorted and unbalanced isolated SEIG environment of this study [11]. Table 2.1 presents the comparative performance benchmarking of these methods. Table 2.1 Comparative Analysis of PLL and Synchronisation Techniques

Synchronisation Method	Harmonic Rejection	DC Offset Immunity	Unbalance Handling	Complexity
SRF-PLL	Poor	Poor	Poor	Low
SOGI-PLL	Moderate	Moderate	Moderate	Medium
DSOGI -FLL	Good	Good	Good	Medium
MFLL	Very Good	Good	Good	High
DTOGI-PLL	Excellent	Excellent	Excellent	Medium High

2.6 ANFIS-Based Intelligent Control for Power Systems

A five-layer feed-forward network architecture integrating Takagi-Sugeno fuzzy inference with a hybrid gradient-descent and least-squares neural network learning algorithm was introduced for complex nonlinear system modelling and control, demonstrating faster convergence and better generalisation than pure backpropagation the ANFIS framework subsequently adopted in the present frequency controller [13]. The suitability of ANFIS for power electronic control was identified on the basis of its ability to model complex nonlinear input-output mappings with compact network structures while maintaining interpretability through the underlying fuzzy rule structure [14]. The critical advantage of ANFIS over fixed-parameter PI controllers in isolated microgrid frequency regulation arises from its nonlinear, operating-point-dependent control law: under large disturbances it delivers strong corrective action to arrest frequency deviation rapidly, whilst under small perturbations it avoids the overshoot and oscillation characteristic of high-gain PI controllers [13]. In the proposed system, frequency error $e(k) = f^* - f(k)$ and its rate of change $\Delta e(k) = e(k) - e(k-1)$ serve as the two ANFIS inputs, producing a correction signal that adjusts the BDC battery current reference to converge frequency within ±0.15 Hz of the 50 Hz nominal and below 0.01 Hz steady-state error representing a 57% reduction in post-disturbance ROCOF relative to conventional SRF-PLL-based control [12], [13].

2.7 Harmonic Mitigation and IEEE Standard 1547 Compliance

Harmonic mitigation strategies in distribution networks span passive filters, active power filters, and hybrid configurations; passive approaches are constrained by fixed tuning and impedance sensitivity, whilst active power filters overcome these limitations through dynamic harmonic extraction and injection, with effectiveness determined by synchronization accuracy [6]. The p-q theory-based active filter performs comparably to SRF-based approaches under balanced conditions but deteriorates under distorted source voltages [7]. IEEE Standard 1547-2018 mandates a maximum source current THD of 5% at the PCC for all distributed generation interconnections, with individual harmonic limits for orders 3 through 49 [8]. In the proposed system, the uncompensated nonlinear diode bridge rectifier load produces source current THD of 21.4%, with the 5th harmonic at 18.72% and 7th harmonic at 12.38% of fundamental — far exceeding compliance limits. The DTOGI-PLL–ANFIS controlled DSTATCOM reduces source current THD to 2.43%, an 89% reduction achieved with substantial margin below the

IEEE 1547 threshold, surpassing outcomes reported in comparable SRF-PLL-based schemes [9], [12].

2.8 Critical Analysis and Research Gap Identification

A critical synthesis of the reviewed literature exposes four principal deficiencies that collectively define the research problem of this dissertation. First, no prior work has integrated DTOGI-based synchronization with ANFIS frequency control within a unified intelligent control framework for an isolated hybrid PV–Wind–SEIG microgrid; whilst DTOGI-CDSC-FLL control has been demonstrated for grid-connected DG [12] and ANFIS has been applied in simpler configurations [13], their combination for islanded SEIG operation remains entirely unexplored. Second, the SRF-PLL is demonstrably inadequate for DSTATCOM control in isolated SEIG microgrids under nonlinear and unbalanced loads, as documented in [7] and [11], yet its replacement with a DTOGI-based synchronization structure in this specific application context has not been addressed. Third, existing studies treat voltage regulation, frequency control, and harmonic mitigation as isolated objectives; simultaneous achievement of all performance targets voltage regulation, frequency stability, THD $\leq$ 5%, near-unity power factor, and stable DC-link in a single islanded SEIG system under nonlinear loading is absent from the literature [5], [9]. Fourth, quantitative comparative evaluation of DTOGI-ANFIS against SRF-PLL under dynamic load disturbances in an isolated SEIG microgrid, with metrics such as ROCOF, frequency deviation bounds, and transient THD, has not been reported.

2.9 Summary

This chapter has presented a critically evaluated synthesis of literature across all domains pertinent to the present dissertation SEIG modelling, DSTATCOM control, BESS integration, PLL synchronization DTOGI signal processing, ANFIS intelligent control, and IEEE 1547 harmonic compliance. The review has established that, whilst significant individual advances exist in each domain, no prior work has unified DTOGI-PLL synchronization with ANFIS frequency control for the comprehensive power quality regulation of an isolated hybrid PV–Wind–SEIG microgrid under nonlinear and unbalanced loading. The four identified research gaps absence of a unified DTOGI-ANFIS architecture for islanded SEIG systems, SRF-PLL inadequacy under distorted SEIG conditions, lack of simultaneous multi-objective regulation, and missing

quantitative comparative benchmarking collectively define the research problem that the proposed intelligent control framework, detailed in Chapter 3, is designed to resolve.

CHAPTER 3

SYSTEM CONFIGURATION AND CONTROL METHODOLOGY

3.1 Introduction:

The advanced control of isolated hybrid renewable energy systems is essential to ensure reliable operation. It is a control framework that can maintain voltage stability, frequency regulation, and control of harmonics. Under varying load conditions, mitigation, reactive power compensation and dynamic power balancing. operating conditions. With stand-alone microgrids using renewable sources of energy, absence of a stiff utility grid significantly increases the sensitivity of the system towards Nonlinear loading, source intermittencies and transient disturbances. These challenges in SEIG-based systems become more severe due to the presence of the following: The voltage and frequency output are highly sensitive to the value of the excitation capacitance, The rotor speed, and load characteristics. With the proposed hybrid PV–Wind–SEIG micro-grid configuration, the electrical power produced by the PV and wind energy systems are stored in the SEIG. Supplied to a combination of linear and nonlinear loads from a common AC bus. Since the PV system and SEIG with wind-driven system are subjected to the variation of the environment. Under conditions, the power produced is very intermittent. Consequently, significant Voltage fluctuations, frequency deviations, Reactive power imbalance and harmonic distortions are seen at the Point of Common Coupling (PCC). To overcome these limitations, an intelligent coordinated control strategy is designed with the DSTATCOM interfaced Battery Energy Storage System (BESS). Control Systems (PLL) are other key components of the current design. Other key components of the current design include the Energy Storage System (BESS), DTOGI-PLL synchronisation algorithm and ANFIS-based Control Systems (PLL). frequency controller has been implemented.

The proposed control methodology performs the following major functions:

- Synchronisation of the isolated microgrid under distorted conditions.
- Harmonic extraction and compensation
- Voltage regulation at PCC.
- Frequency stabilisation under dynamic loading.
- Active and reactive power balancing.

- DC-link voltage regulation.
- Reference current generation for DSTATCOM.
- Battery charging/discharging coordination.
- Extraction of maximum solar power using MPPT.
- Maintenance of IEEE-1547 harmonic compliance.

The overall control system is designed in MATLAB/Simulink with a discrete with a sampling time of 5 ×10−6 s. The proposed intelligent controller combines the performance of Dual Third-Order Generalized Integrator Phase-Locked Loop. With adaptive learning capabilities of the Adaptive Neuro-Fuzzy Inference (DTOGI-PLL). The paper presents the use of Artificial Neural Network (ANFIS) to enhance the dynamic response and power quality under severe periodic load changes. operating disturbances.

3.2 Overall System Configuration

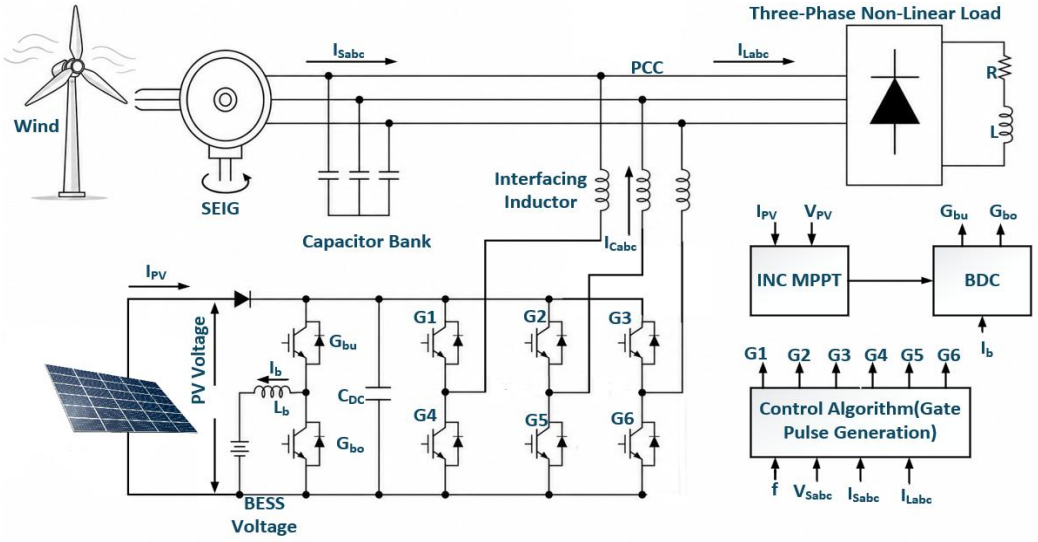

Fig.3.1 Configuration of distributed wind–PV microgrid system

TABLE 3.1
Machine Rating & Parameters of The Proposed Wind-PV Microgrid Configuration

S.No.	Quantity	Parameters
1.	SEIG and interfacing inductors	3-ϕ, 4-Pole, 3.73 kW, 415 V, 50 Hz, Y connected.R_s = 1.405 Ω, R_r = 1.39 Ω, L_s = L_r = 7.8 mH, Inertia = 0.138 J(Kg.m^2), Friction factor = 0 F (N .m .s), Pole pairs = 2

2.	SPV array	V_{PV} = 210V, I_{PV} = 12A
3.	BESS	400 V, 7.5 Ah
4.	Non-linear Load	R = 18 Ω, L = 0.12 H
5.	Controller parameters	PI controller – in V_t control loop, k_p = 0.5 and k_i = 6
6.	Temperature	35° - 20° C
7.	Wind Speed	19 m/s
8.	Irradiance	1000 W/m^2 – 750 W/m^2

The proposed isolated hybrid renewable energy system consists of the following subsystems:

- Wind turbine-driven SEIG
- Solar photovoltaic (SPV) array
- Battery Energy Storage System (BESS)
- DSTATCOM-based Voltage Source Converter (VSC)
- Bidirectional DC–DC converter
- Nonlinear load
- DTOGI-PLL synchronisation controller
- ANFIS frequency controller
- Hysteresis Current Controller (HCC)

The Table 3.1 signifies the system parameters and specifications of the model, which is prescribed in the Fig. 3.1. The overall system architecture is based on a three-phase three-wire isolated microgrid arrangement. The main generation unit is the SEIG driven by a variable speed wind turbine. The extra active power is injected by SPV system through Boost Converter controlled by INC MPPT technique.

The Battery Energy Storage System is connected to the common DC-link through a bidirectional DC–DC converter. The BESS is to keep the power balance in case of fluctuations of renewable power and load transients. The DSTATCOM injects compensating currents in the PCC for suppression of harmonics and reactive power support.

The nonlinear load is modelled as three phase uncontrolled diode bridge rectifier feeding RL load which add significant harmonic distortion to the system.

The proposed controller continuously monitors:

- Source voltage

- Source current
- Load current
- Converter current
- DC-link voltage
- Battery current
- Frequency

Based on these measured signals, the controller generates switching pulses for the VSC.

3.3 Introduction of Proposed Control Methodology

The proposed control methodology integrates:

- DTOGI-PLL synchronisation technique
- ANFIS-based intelligent frequency controller
- DSTATCOM current compensation
- BESS coordinated control
- INC-MPPT-based PV power extraction

The control algorithm is composed of harmonic filtering and positive sequence extraction under distorted operation conditions.

Stage 1: Signal Acquisition

The following signals are continuously sensed:

- Source voltages
- Source currents
- Converter currents
- Load currents
- DC-link voltage
- Battery current

These measured quantities form the input to the controller.

Stage 2: Clarke Transformation

The three-phase signals are converted into components of stationary reference frame. The Clarke transformation equations are:

$$\begin{bmatrix} i_\alpha \\ i_\beta \end{bmatrix} = \frac{2}{3} \begin{bmatrix} 1 & -\frac{1}{2} & -\frac{1}{2} \\ 0 & \frac{\sqrt{3}}{2} & -\frac{\sqrt{3}}{2} \end{bmatrix} \begin{bmatrix} i_a \\ i_b \\ i_c \end{bmatrix} \quad (3.1)$$

Stage 3: DTOGI Filtering

The DTOGI filter extracts:

- Fundamental component
- Positive sequence component
- Quadrature signals

The DTOGI filter effectively rejects:

- Harmonics
- DC-offset
- Noise
- Unbalance

Stage 4: PLL Synchronisation

The PLL estimates:

- Frequency
- Phase angle
- Grid synchronisation variables

Stage 5: ANFIS Frequency Control

The ANFIS controller processes:

- Frequency error
- Change in frequency error

It generates adaptive frequency correction signals.

Unlike conventional controllers, ANFIS continuously updates control behaviour based on operating conditions.

Stage 6: Unit Vector Generation

In-phase and quadrature unit templates are generated for:

- Active current extraction
- Reactive current extraction
- Reference current generation

Stage 7: Reference Current Calculation

Reference compensating currents are calculated for:

- Harmonic elimination
- Reactive power compensation
- Current balancing

Stage 8: Hysteresis Current Control

The HCC compares:

- Actual source current
- Reference source current

Advantages of Proposed Control Methodology

The proposed control offers:

- Fast synchronisation
- Low steady-state error
- Excellent harmonic suppression
- Frequency stability
- Better disturbance rejection
- Adaptive control performance
- Robust operation under nonlinear loading

3.4 DSTATCOM and DC-Link Capacitor

The Distributed Static Compensator (DSTATCOM) is a shunt connected custom power device widely used in modern power systems for enhancing power quality and maintaining system stability under different operating conditions. Standalone renewable energy based microgrid with nonlinear loads and intermittent generation creates serious challenges like voltage fluctuation, reactive power imbalance, harmonic distortion and low power factor. These problems are more pronounced in Self-Excited Induction Generator (SEIG) based systems as the generated voltage and frequency are highly dependent on load characteristics and excitation conditions. Therefore, a DSTATCOM is used in the proposed hybrid PV–Wind–SEIG microgrid for the instantaneous compensation of reactive power demand and mitigation of power quality disturbances at the Point of Common Coupling (PCC).

The DC-link capacitor is the energy storage element on the DC side of the Voltage Source Converter (VSC) and is critical to the stable operation of the converter. It is an intermediate energy reservoir between the AC and DC parts of the system. The capacitor stores energy when there is an excess of power generation and releases energy

when additional power is needed for compensation. The energy exchange between the converter and the AC system is continuous and consequently the DC-link voltage will naturally fluctuate. Therefore, the current compensation and proper operation of the converter require a constant DC-link voltage.

The DC-link capacitor also supplies the active power needed to compensate for the switching losses in the converter, and to meet the transient power demands during abrupt changes in load conditions or renewable generation. If the DC-link voltage is too far from its reference value, the converter may fail to create the required compensating voltages and currents, thus resulting in poor harmonic cancellation and degradation in dynamic performance. As a result, a control loop is used to continuously measure and control the DC-link voltage around its reference.

The proposed control architecture is based on a Battery Energy Storage System (BESS) connected to the common DC-link through a bidirectional DC-DC converter. The BESS and DC-link capacitor are coordinated to work together to improve the system stability by balancing the power during the fluctuating wind and solar generation. In the excess renewable power period, the battery stores the excess power and charges the DC-link, and in the power deficit period, the battery discharges and provides the required active power. The coordinated control greatly improves the transient response, reduces the frequency deviations, enhances the voltage regulation ability, and allows the isolated microgrid to operate stably under dynamic loading conditions.

Hence, the proposed power conditioning scheme is based on the combined operation of the DSTATCOM and DC-link capacitor, which ensures effective reactive power support, harmonic compensation, voltage stabilisation and improved power quality performance in the isolated hybrid PV–Wind–SEIG microgrid.

3.5 DTOGI-PLL Synchronization Technique

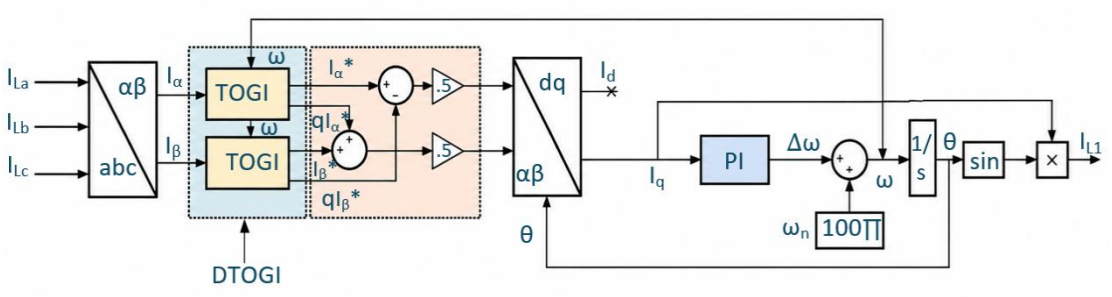

Fig.3.2 DTOGI-PLL Control Algorithm

The fig.3.2 showcases the implemented control algorithm required for the model, which is illustrated in fig.3.1. The synchronisation unit is an important part in both grid connected and isolated distributed generation systems in order to determine the correct value of frequency, phase angle, and amplitude of fundamental component of the system under different operating conditions. When measuring the voltage and current waveforms in a hybrid renewable energy system (such as a standalone microgrid with nonlinear loads and variable renewable generation), harmonics, unbalance, switching noise, and DC offset are common sources of distortion. The conventional synchronisation methods like the Synchronous Reference Frame Phase-Locked Loop (SRF-PLL) do not perform well in the presence of these conditions due to the presence of oscillations and inaccuracy in frequency estimation. Thus, an advanced synchronisation technique using Dual Third-Order Generalized Integrator Phase-Locked Loop (DTOGI-PLL) is used to synchronise the proposed microgrid system.

The main function of the DTOGI-PLL is to isolate the basic positive sequence component of the distorted current signal and to generate accurate values of frequency and phase needed for the reference current generation in the control system of the DSTATCOM. Compared to the conventional PLL structures, DTOGI-PLL has enhanced harmonic filtering ability, DC-offset rejection characteristics and enhanced dynamic response under transient operating condition. This method automatically adjusts itself to frequency changes and generates good synchronization under severe nonlinear loading conditions

The general idea behind DTOGI-PLL is that three phase measured signals are converted to stationary reference frame quantities, filtered through Third-Order Generalized Integrator (TOGI) filters, and then sent to the PLL. The DTOGI filter produces in-phase and quadrature signals and these are then processed to obtain the positive sequence components.

First the measured three phases are transformed to stationary reference frame αβ according to Clarke transformation:

$$\begin{bmatrix} i_\alpha \\ i_\beta \end{bmatrix} = \frac{2}{3} \begin{bmatrix} 1 & -\frac{1}{2} & -\frac{1}{2} \\ 0 & \frac{\sqrt{3}}{2} & -\frac{\sqrt{3}}{2} \end{bmatrix} \begin{bmatrix} i_a \\ i_b \\ i_c \end{bmatrix} \quad (3.2)$$

Where:

i_a, i_b and i_c are three phase currents.

i_α, i_β are stationary current components.

The DTOGI filter is then applied on the filtered signals. The transfer function of Third-Order Generalized Integrator can be expressed as:

$$H(S) = \frac{N(S)}{S^3+a_2S^2+a_1S+a_o} \quad (3.3)$$

where $N(s) = Kw_os^2$

- K = gain constant
- ω_0= fundamental angular frequency
- a_1, a_2= filter parameters determining bandwidth

The TOGI filters are used to obtain the filtered i_α and i_β currents (i_α^1 and i_β^1) as well as their quadrature values (qi_α^1 and qi_β^1). The transfer function is written as for the filter.

The transfer function for the in-phase component of DTOGI is given by:

$$D(s) = \frac{i_{\alpha,\beta}^1}{i_{\alpha,\beta}} = \frac{a_1w^2s}{s^3+a_2ws^2+(a_1+1)w^2s+a_2w^3} \quad (3.4)$$

Similarly, the quadrature signal transfer function becomes:

$$Q(s) = \frac{qi_{\alpha,\beta}^1}{i_{\alpha,\beta}} = \frac{w}{s}D(s) = \frac{a_1w^2s}{s^3+a_2ws^2+(a_1+1)w^2s+a_2w^3} \quad (3.5)$$

The DTOGI filter generates:

- Filtered in-phase signals: i_α^1 and i_β^1
- Filtered quadrature signals: qi_α^1 and qi_β^1

The filtered signals are then processed with the Positive Sequence Evaluator (PSE) to get the components of the fundamental frequency positive sequence (FFPS). The positive sequence extraction equations are:

$$i_\alpha^+ = 0.5(i'_\alpha - qi'_\beta) \quad (3.6)$$
$$i_\beta^+ = 0.5(i'_\beta + qi'_\alpha) \quad (3.7)$$

The extracted positive sequence components will only have fundamental balanced quantities and will not contain the harmonic or the negative sequence components.

The extracted signals are then converted to the rotating dq synchronous reference frame as follows:

$$\begin{bmatrix} i_d \\ i_q \end{bmatrix} = \begin{bmatrix} \cos\theta & \sin\theta \\ -\sin\theta & \cos\theta \end{bmatrix} \begin{bmatrix} i_\alpha^+ \\ i_\beta^+ \end{bmatrix} \quad (3.8)$$

Where :

- i_d = direct-axis component
- i_q = quadrature-axis component
- θ = estimated phase angle

The direct-axis component represents the active power component, whereas the quadrature-axis component represents the reactive power component.

The PLL performs frequency estimation in the system using the quadrature axis component in a control loop estimation.

The phase angle is calculated by numerical integration of the estimated angular frequency:

$$\theta = \int w dt \quad (3.9)$$

The angular frequency is related to system frequency as:

$$w = 2\pi f \quad (3.10)$$

The coordinate transformation process is continuously estimated by the phase angle, so that a closed-loop synchronisation mechanism is formed.

The complete DTOGI-PLL operation can be summarised in the following sequence:

Step 1: Measure three-phase voltages and currents at PCC.

Step 1: Measure three-phase voltages and currents at PCC.

Step 2: Apply Clarke transformation to obtain αβ components.

Step 3: Pass αβ components through DTOGI filter.

Step 4: Generate in-phase and quadrature filtered signals.

Step 5: Extract positive sequence fundamental components.

Step 6: Transform positive sequence components into d_q frame.

Step 7: Estimate phase angle and frequency.

Step 8: Generate synchronisation signals for reference current computation.

The major advantages of DTOGI-PLL over conventional SRF-PLL include:

- Better harmonic rejection capability
- Effective DC-offset elimination
- Reduced steady-state oscillation
- Fast dynamic response
- Improved frequency estimation accuracy
- Robust performance under unbalanced loading

- Enhanced synchronisation under distorted operating conditions

Thus, the DTOGI-PLL synchronisation technique significantly enhances the performance of the DSTATCOM control system, and guarantees stable operation of the isolated hybrid PV–Wind–SEIG microgrid under various operating conditions.

3.6 Adaptive Neuro Fuzzy Inference System (ANFIS)

Adaptive Neuro-Fuzzy Inference System (ANFIS) is an intelligent control technique, which combines the learning capability of Artificial Neural Networks (ANN) and fuzzy logic reasoning capability of Fuzzy Logic Systems (FLS). Combining the two methodologies allows the controller to handle the nonlinear and uncertain system which, in particular cases, may be hard to obtain the exact mathematical representation. The operating conditions of Self-Excited Induction Generator (SEIG), the wind speed, and solar irradiance, as well as the nonlinear load demand, continuously change in renewable energy based isolated microgrids. Therefore, the control performance of conventional controllers such as Proportional-Integral (PI) controllers can be insufficient in some cases, because the gains of the controllers are fixed irrespective of operating conditions.

The ANFIS controller overcomes these limitations by adjusting the parameters of the controller based on the changing conditions of the system. It is constantly learning from system behaviour and adjusting the control output to reduce the error. As the frequency deviation is very sensitive to the renewable power fluctuations and load disturbances, ANFIS is used for frequency regulation in the proposed hybrid PV–Wind–SEIG microgrid.

The ANFIS controller receives two input variables:

- Frequency error
- Change in frequency error

The frequency error is defined as: $e(k) = f^* - f(k)$ (3.11)

Where:

f^* = reference frequency (50 Hz)

$f(k)$ = measured system frequency

The change in frequency error is expressed as:

$$\Delta e(k) = e(k) - e(k-1) \quad (3.12)$$

Where:

$e(k-1)$ = previous frequency error

The output of ANFIS generates a control signal for frequency correction.

The ANFIS architecture generally consists of five layers:

Layer 1: Fuzzification layer

Input variables are converted into fuzzy quantities.

Layer 2: Rule layer

Firing strengths of fuzzy rules are computed.

Layer 3: Normalisation layer

Rule strengths are normalised.

Layer 4: Defuzzification layer

Individual rule outputs are generated.

Layer 5: Output layer

Overall output is computed.

The ANFIS output is used to regulate the microgrid frequency under dynamic operating conditions.

3.6.1 Membership Function

The membership function is one of the key components of the Adaptive Neuro-Fuzzy Inference System (ANFIS) which is used to transform numerical inputs into fuzzy linguistic variables for decision making. The ANFIS controller uses the frequency error and frequency error change as the input variables for the proposed hybrid PV–Wind–

SEIG microgrid. If these signals are directly processed, the continuous change of these inputs caused by the variations of the renewable generation and load conditions may not lead to accurate control action.

In the proposed ANFIS controller, Gaussian membership functions are used because they provide:

- Smooth nonlinear transition
- Better learning capability
- Continuous differentiability
- Fast convergence
- Improved stability

Membership function shows the degree of the input variable belonging to the fuzzy set. In classical logic a value is either a member of a set or it is not in the set but in fuzzy logic partial membership is possible in the range.

$$0 \leq \mu(x) \leq 1 \qquad (3.13)$$

Where:

- $\mu(x)$ = degree of membership
- x = input variable

If:

- $\mu(x) = 0$, the variable does not belong to the fuzzy set.
- $\mu(x) = 1$, the variable completely belongs to the fuzzy set.
- $0 < \mu(x) < 1$, the variable partially belongs to the fuzzy set.

For example, if the microgrid frequency error is very small, the controller can identify it as “Zero” or “Positive Small” with different degrees of membership. Therefore, the ANFIS controller provides a smooth and continuous control behavior, rather than abrupt changes in control action.

The performance of the controller depends largely on the choice of an appropriate membership function since it decides the sensitivity and learning ability of the system. An incorrect choice of a membership function may lead to an increase of the steady state error, oscillations and a decrease of the system stability. Therefore, membership

functions need to be appropriately chosen according to the nature of the application and system dynamics.

3.6.2 Rule Base Design

The design of the rule base is regarded as the decision-making part of the Adaptive Neuro-Fuzzy Inference System (ANFIS). It employs a set of fuzzy IF-THEN rules to define a logical relationship between the input variables and the corresponding output control action. The main purpose of the rule base is to understand the operating condition of the system and then provide an appropriate control response. The frequency error and change in frequency error are given to the ANFIS rule base for producing a corrective signal to control the frequency for the proposed hybrid PV – Wind – SEIG microgrid.

The performance of the ANFIS controller is very sensitive to the optimal design of the rule base determining the controller response under different operating conditions. The rule base is the knowledge of the system, expressed in the form of linguistic description, and simulates the reasoning behaviour of human decision makers in uncertain and nonlinear environments. The hybrid microgrid is subjected to time-varying conditions due to the fluctuation of wind speed, solar irradiance, and load demand. Hence, the rule base offers an adaptive control action without an accurate mathematical model.

The ANFIS proposed is based on the sugeno-type fuzzy inference due to its simple structure, low computation, and suitability for adaptive learning applications. In this method, each fuzzy rule is composed of an antecedent part and a consequent part. The antecedent part describes the input conditions, while the consequent part specifies the corresponding output action.

3.6.3 ANFIS Training Process

The training process of Adaptive Neuro-Fuzzy Inference System (ANFIS) is used to build the learning capability of the controller by adjusting automatically the internal parameters of the controller according to the operating behaviour of the system. The main objective of the training procedure is to obtain an optimum nonlinear relationship between the input variables and the output control action which will allow the controller

to respond to various operating conditions. The proposed hybrid system comprised of PV–Wind–SEIG microgrid is implemented, which is trained by the ANFIS controller for the regulation of the system frequency under different renewable generations and loads. The controllers of a fixed parameter type are not able to ensure satisfactory performance for all operating conditions because the operation of renewable energy systems is nonlinear and uncertain. Thus, ANFIS has an adaptive learning mechanism that fine-tunes its parameters on the basis of the observed system behaviour.

To train the ANFIS model, a massive dataset of the input-output values is gathered from microgrid dynamic operations under different loads, wind speed variations, solar irradiance changes, and transient disturbances. Frequency error and change in frequency error are considered as the input variables for the proposed controller and the output variable is the control signal for frequency correction required. In training, the ANFIS controller examines the relationship between the above variables and decides upon the most appropriate fuzzy inference structure to describe the system behavior.

The learning process of ANFIS is a combination of the properties of artificial neural network and fuzzy logic system. Neural networks can learn patterns from data, and fuzzy systems can have decision-making capability based on linguistic rules. In the learning algorithm, both the parameters of the premise of the membership functions and the parameters of the consequent of the fuzzy rules are adjusted. Hence, the controller continues to get better at predicting the outputs and reduces the difference between the actual output and the desired output.

3.7 Voltage Amplitude Evaluation and Unit Template Generation

Because they provide the necessary synchronization signals for reference current production and coordinated control of the DSTATCOM, voltage amplitude evaluation and unit template creation are crucial components of the suggested control approach. This procedure's goal is to produce normalized sinusoidal unit vectors that, under various operating circumstances, stay in sync with the system voltage. In order to calculate reference source current, these unit vectors are also used in the extraction of active and reactive current components.

The observed three-phase voltages at the Point of Common Coupling (PCC) in the proposed hybrid PV–Wind–SEIG microgrid may be affected by nonlinear loads, variations in renewable power, and brief disruptions. Therefore, the controller has to ascertain the true size of the basic voltage component before creating unit templates. Precise estimate of voltage amplitude guarantees appropriate reference current generation and enhances the efficiency of voltage control and harmonic correction.

Initially, the three-phase instantaneous voltages at PCC are represented as:

v_a = voltage of phase a

v_b = voltage of phase b

v_c = voltage of phase c

The instantaneous voltage amplitude of the three-phase system is evaluated as:

$$V_t = \sqrt{0.666(v_{sa}^2 + v_{sb}^2 + v_{sc}^2)} \tag{3.14}$$

Where:

V_t = instantaneous terminal voltage magnitude

By computing the root mean square equivalent value of the three-phase voltages, the aforementioned equation establishes the magnitude of the basic voltage component. The controller continually updates the computed voltage amplitude to enable precise tracking of fluctuations brought on by shifting operating circumstances.

The observed phase voltages are normalized to produce in-phase unit vectors once the voltage magnitude has been assessed. Sinusoidal signals with unit magnitude and the same phase as the system voltages are represented by these unit vectors.

The instantaneous voltages are divided by the voltage amplitude (V_t) to get the unit vectors:

$$\left.\begin{aligned} U_{pa} &= \frac{v_{sa}}{V_t} \\ U_{pb} &= \frac{v_{sb}}{V_t} \\ U_{pc} &= \frac{v_{sc}}{V_t} \end{aligned}\right\} \tag{3.15}$$

U_{pa}, U_{pb}, U_{pc} are in-phase unit vectors.

In-phase vectors are used to compute the quadrature unit's voltage templates, which are then assessed as follows:

$$\left.\begin{aligned} U_{qa} &= (-U_{pb} + U_{pc})/\sqrt{3} \\ U_{qb} &= (3U_{pa} + U_{pb} - U_{pc}) / 2\sqrt{3} \\ U_{qc} &= (-3U_{pa} + U_{pb} - U_{pc}) / 2\sqrt{3} \end{aligned}\right\} \quad (3.16)$$

U_{qa}, U_{qb}, U_{qc} are quadrature unit vectors

The reactive component of current is represented by the quadrature unit vectors, which are orthogonal to the in-phase unit vectors. The phase shift needed for reactive power compensation is provided by these vectors.

In the coordinated control process, the created unit templates are crucial. The respective current magnitudes are multiplied by these unit vectors to generate the active and reactive components of reference source currents.

The active reference current component is obtained as:

$$i_p^* = I_p U_{pa} \quad (3.17)$$

Similarly, the reactive reference current component becomes:

$$i_q^* = I_q U_{qa} \quad (3.18)$$

The total reference source current is therefore expressed as:

$$i_s^* = i_p^* + i_q^* \quad (3.19)$$

The Hysteresis Current Controller is then used to create switching pulses for the Voltage Source Converter using the generated reference currents.

The use of voltage amplitude estimation and unit template generation offers several advantages in the proposed microgrid:

- Accurate synchronisation under distorted conditions
- Improved harmonic compensation
- Better reactive power control
- Stable voltage regulation
- Reduced current distortion
- Enhanced converter current tracking capability
- Improved dynamic response

3.8 Gate Pulse Generation

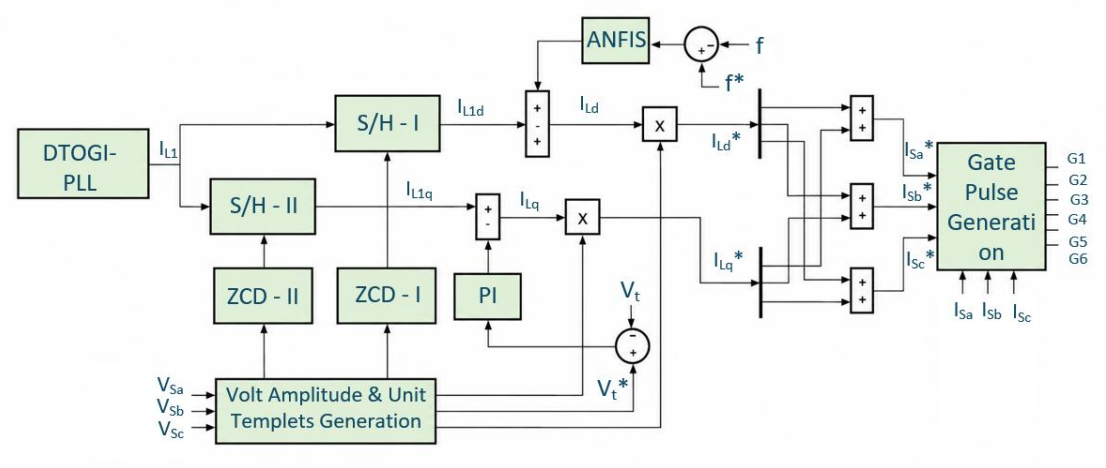

Fig.3.3 Pulse Generation

The fig.3.3 showcases the gate pulse generation required for the model, which is illustrated in fig.3.1Because it regulates the switching function of the Voltage Source Converter (VSC)-based DSTATCOM and assesses the efficacy of current compensation in the hybrid PV–Wind–SEIG isolated microgrid, the gate pulse generating process is an important component of the suggested control approach. In order for the DSTATCOM to inject the proper compensatory currents into the Point of Common Coupling (PCC) for harmonic reduction, reactive power compensation, voltage regulation, and frequency stabilization, the produced switching pulses control the functioning of converter switches.

Before producing the final switching signals, the recorded electrical variables are processed through many steps by the gate pulse generation mechanism used in the suggested system, which employs a coordinated control technique. The adaptive hybrid filtering step receives the distorted source and load current signals first, reducing noise disturbances and harmonic components. Before creating reference currents, the fundamental component must be extracted since nonlinear loading circumstances cause the measured currents to have both fundamental and harmonic components.

The controller uses Sample-and-Hold (S/H) circuits and Zero Crossing Detectors (ZCDs) to accurately extract the basic current component after the filtering step. The Zero Crossing Detector continually scans the input waveform to identify the moment the signal crosses the zero-reference axis and changes polarity. Because they show the start and finish of one & half cycle of the signal waveform, these zero-crossing instants

are significant. The control signals produced by the identified crossing locations synchronize the Sample-and-Hold circuits' operations.

During each running cycle, the peak value of the filtered current signal is recorded and stored by the Sample-and-Hold circuit. The Sample-and-Hold block records the associated signal value and keeps it constant until the next sampling moment happens after the Zero Crossing Detector determines the proper sampling instant. This method lessens the impact of harmonics and high-frequency disturbances while accurately extracting the basic active and reactive current components. As a result, the controller receives steady, smooth current indications that may be processed further.

The synchronization signals from the DTOGI-PLL unit are then mixed with the extracted current components. Synchronized in-phase and quadrature unit vectors that stay in line with the basic system voltage are provided by the DTOGI-PLL. These unit vectors help separate the components of active and reactive current while maintaining phase information. While the reactive current component is linked to voltage management and reactive power compensation, the active current component is linked to actual power transfer and frequency regulation.

The ANFIS controller receives the frequency error that results from the system's continual comparison of the frequency data with the reference frequency. After processing this mistake, the ANFIS controller produces an adaptive correction signal based on the operating circumstances of the system. In contrast to traditional fixed-gain controllers, the ANFIS controller enhances dynamic responsiveness by adjusting its output in reaction to changes in system behavior.

13 The instantaneous reference source currents are obtained by multiplying the active and reactive current components produced by the control mechanism by their corresponding in-phase and quadrature unit templates. The optimal source current waveforms that should pass through the system under compensated operating circumstances are represented by these reference currents.

72 The Hysteresis Current Controller (HCC) receives the produced reference currents and compares them to the source currents. In order to keep the inaccuracy within the upper and lower hysteresis limits, the HCC continually measures the difference between the real and reference currents. Switching instructions are instantly produced for the converter switches once the current error surpasses these limits.

As a result, the pulse generating mechanism continually modifies the switching states

15 of the Voltage Source Converter's six IGBT devices. To ensure that the converter output

current precisely matches the reference current trajectory, the controller turns individual switches ON or OFF based on the immediate magnitude of current error. The DSTATCOM can dynamically inject the necessary compensatory current into the PCC thanks to this procedure.

Accurate gate pulse generation under various operating situations is ensured by the coordinated functioning of the adaptive filter, Zero Crossing Detector, Sample-and-Hold circuit, DTOGI–PLL synchronization unit, ANFIS controller, and Hysteresis Current Controller. The suggested hybrid PV-Wind-SEIG isolated microgrid's overall power quality performance is much improved by this coordinated control structure, which also reduces harmonic distortion, increases dynamic responsiveness, and improves current tracking capabilities.

3.9 MPPT Control Method for SPV Generation

One of the main renewable energy sources used in the proposed hybrid PV–Wind–SEIG microgrid to provide active power to the load and enhance overall system dependability is the Solar Photovoltaic (SPV) system. However, environmental factors like sun irradiation and cell temperature have a significant impact on a photovoltaic array's output characteristics. The voltage and current produced by the PV array are constantly changed by variations in these parameters, resulting in variations in output power. As a result, the energy utilization efficiency is decreased since the photovoltaic system does not always run at its maximum power point.

The suggested approach uses a Maximum Power Point Tracking (MPPT) technique to get around this restriction. Regardless of shifting meteorological circumstances, the MPPT controller's main goal is to constantly harvest the most power possible from the solar array. By regulating the duty cycle of the DC–DC boost converter linked between the PV system and the common DC-link, the MPPT algorithm continually modifies the PV array's operational point.

A photovoltaic array's power-voltage characteristic is nonlinear and has a special operating point called the Maximum Power Point (MPP), where the output power produced reaches its maximum. Power production is reduced when this operational point is deviated from. As a result, the MPPT controller moves the operating point in the direction of the maximum power area while continually monitoring the PV voltage and current.

The Incremental Conductance (INC) MPPT approach is used in the proposed hybrid microgrid system because to its enhanced tracking capabilities and increased performance under situations of rapidly changing irradiance. The Incremental Conductance approach reduces oscillations around the operating point and offers quicker convergence towards the maximum power point.

The slope of the PV power-voltage characteristic curve serves as the foundation for the Incremental Conductance algorithm's fundamental working concept. The power curve's slope drops to zero at the highest power point. Consequently, the link between incremental conductance and instantaneous conductance may be used to estimate the PV system's working state.

The PV array, which is intended to provide 3.6 kW of electricity, consists of six series and two parallel modules. When solar irradiance fluctuates, the BDC converter is controlled by an INC-based MPPT algorithm while the VSC maintains the DC link voltage (vdc) at 400 V. The following relation is used to determine the buck boost converter's duty cycle (DC):

$$DC = 1 - {V_{dc}}/{V_{pv}} \tag{3.20}$$

Here, the output voltage of the maximum power point tracking(MPPT) controller based on the incremental conductance(INC) technique is denoted by V_{pv}. The incremental conductance (INC) technique generates the duty cycle for the bidirectional DC-DC converter(BDC). The maximum power point (MPPT) can be determined using the following relationship;

$$\frac{dP'}{dV'} = \frac{d(V' * I')}{dV'} = I' + V' \frac{dI'}{dV'} \tag{3.21}$$

The value of MPP when $\frac{dP'}{dV'}$ and $\frac{dI'}{dV'} = -\frac{I'}{V'}$:

$$\frac{dP'}{dV'} > 0 \text{ then } V_p' < V_{mpp}'$$

$$\frac{dP'}{dV'} = 0 \text{ then } V_p' = V_{mpp}'$$

$$\frac{dP'}{dV'} < 0 \text{ then } V_p' > V_{mpp}'$$

3.10 BDC control Strategy

Under varying operating conditions of the proposed hybrid PV–Wind–SEIG microgrid, the generated power from renewable sources continuously changes because of fluctuations in wind speed and solar irradiance. Since renewable generation is inherently intermittent, the generated power may not always match the load demand. During excess power generation conditions, surplus energy becomes available within the system, whereas during insufficient generation conditions, power deficiency occurs. These variations may produce voltage fluctuations, frequency deviations, and instability in the DC-link voltage. Therefore, a Battery Energy Storage System (BESS) integrated through a bidirectional DC–DC converter (BDC) is employed to maintain power balance and ensure stable operation of the microgrid.

The Battery Energy Storage System acts as an energy balancing unit by storing excess energy during low demand conditions and supplying stored energy during high demand periods. The bidirectional DC–DC converter provides controlled power exchange between the battery and the common DC-link. The converter operates in two different modes depending upon system requirements:

- Battery charging mode
- Battery discharging mode

During excess renewable generation conditions, when generated power exceeds load demand, the DC-link voltage tends to increase because additional energy accumulates on the DC side. Under this condition, the bidirectional converter operates in charging mode and transfers excess energy from the DC-link to the battery. Consequently, battery charging takes place and the DC-link voltage is restored to its reference value.

Conversely, during insufficient renewable generation conditions or sudden load increase, the DC-link voltage begins to decrease due to increased power demand. Under such operating conditions, the bidirectional converter changes its mode of operation and allows the battery to discharge its stored energy into the DC-link. This process supports system power requirements and stabilises the DC-link voltage.

Therefore, the bidirectional converter acts as an intelligent interface between the battery and DC-link by regulating the direction and magnitude of power flow according to system operating conditions.

The control strategy of the Battery Energy Storage System is primarily based on maintaining a constant DC-link voltage because stable DC-link operation is essential for proper functioning of the Voltage Source Converter (VSC). Any significant deviation in DC-link voltage affects converter output voltage generation and consequently deteriorates current compensation performance.

The actual DC-link voltage is continuously measured and compared with the reference DC-link voltage to determine the voltage deviation present within the system. This deviation indicates the amount of additional power required to maintain system stability.

The DC-link voltage error is obtained as:

$$V'_{dce}(s) = V'_{dcref}(s-1) - V'_{dc}(s) \quad (3.22)$$

Where:

- V'_{dcref} = reference DC-link voltage
- V'_{dc} = measured DC-link voltage
- V'_{dce} = DC-link voltage error

The generated error signal is subsequently processed through a Proportional–Integral (PI) controller. The PI controller continuously monitors both the present value of voltage error and accumulated past error in order to minimise deviations effectively. The control equations for the BDC are presented below:

$$i'_{bref}(s) = i'_{bref}(s-1) + k_p(V''_{dce}(s) - V'_{dce}(s-1)) + k_i V'_{dce}(s) \quad (3.23)$$

Where, k_p and k_i are the gain of PI controller.

The proportional term improves transient response by reacting immediately to changes in DC-link voltage, whereas the integral term eliminates steady-state error by considering accumulated error over time. The generated reference current determines the amount of charging or discharging current required from the battery. The actual battery current is continuously monitored and compared with the generated reference current. The difference between these currents produces battery current error:

$$i_{ber} = i_{bref} - i_b \quad (3.24)$$

Where:

- i_{ber} = battery current error
- i_b = actual battery current
- i_{bref} = battery reference current

The proportional term improves transient response by reacting immediately to changes in DC-link voltage, whereas the integral term eliminates steady-state error by considering accumulated error over time.

The duty cycle controls the switching operation of the bidirectional converter and determines the magnitude as well as direction of power flow.

When: $i_{bref} > 0$, the converter operates in charging mode and power flows from the DC-link to the battery.

When: $i_{bref} < 0$, the converter operates in discharging mode and power flows from the battery to the DC-link.

Thus, the Battery Energy Storage System continuously regulates the DC-link voltage and compensates for power mismatch between renewable generation and load demand. The coordinated operation of the BESS with the DSTATCOM improves:

- DC-link voltage stability
- Frequency regulation capability
- Dynamic response
- Renewable power utilisation
- Power balancing
- Transient stability
- Overall microgrid reliability

Hence, the bidirectional DC–DC converter and Battery Energy Storage System play a crucial role in maintaining stable operation of the isolated hybrid PV–Wind–SEIG microgrid under dynamic operating conditions.

CHAPTER 4

RESULT AND DISCUSSION

4.1 Introduction

This chapter presents the detailed simulation results and performance analysis of the proposed hybrid PV–Wind–SEIG isolated microgrid integrated with a DSTATCOM-assisted Battery Energy Storage System (BESS), DTOGI-PLL synchronisation technique, and ANFIS-based control strategy. The complete system was modelled and simulated in the MATLAB/Simulink environment to evaluate its dynamic behaviour and control effectiveness under various operating conditions. The simulation analysis was performed considering both steady-state and transient operating scenarios with nonlinear load variations in order to validate the robustness and adaptability of the proposed control methodology.

Essential goals for the proposed control system involve keeping the steady functioning of the isolated microgrid. Voltage and frequency are regulated by this mechanism because reactive power demand must be compensated while harmonic distortion is reduced. This control system makes sure that power sharing happens correctly between the renewable energy sources and storage units. Because isolated microgrids face constant changes in generation and load demand, experts claim that keeping power quality and system stability remains a difficult task. Nonlinear loads create more difficulties when these loads bring harmonic currents and frequency changes into the microgrid.

Constant monitoring of system operating conditions is performed by the proposed ANFIS controller. Control signals for the DSTATCOM and BESS interface are adaptively generated by the ANFIS controller. Accurate synchronisation is provided by the DTOGI-PLL when the fundamental component is extracted under distorted operating conditions. It has been observed that the coordinated operation of these components allows for fast fixing of disturbances. This cooperation improves the overall dynamic performance that the microgrid shows.

Findings from the developed model show the system response while nonlinear load disturbances occur during the simulation interval. Performance characteristics are analysed through the use of source voltage, source current, load current, converter

current, DC-link voltage, frequency response, and PV–MPPT variables. The uploaded simulation waveforms show that the source voltage stays balanced with very small changes. While load disturbances happen, the source current keeps sinusoidal characteristics. Many researchers believe that the DC-link voltage stays near the reference value of 400–405 V with very small ripple magnitude because the control system works effectively. Frequency deviations stay close to the nominal 50 Hz value which shows the active power balancing capability of the proposed controller. Tracking of the operating point is successfully demonstrated by the MPPT results even when environmental conditions change.

Harmonic performance analysis and comparative evaluation between conventional PI and ANFIS controllers are carried out to show the effectiveness of the proposed intelligent control strategy. The simulation results confirm that the proposed ANFIS-based approach provides better transient response and less total harmonic distortion. It has been observed that this approach creates better voltage and frequency regulation and higher power quality performance during nonlinear loading conditions. The ANFIS-based approach ensures that the microgrid remains stable.

4.2 MATLAB/Simulink Model Description

Researchers built the hybrid PV–Wind–SEIG isolated microgrid system within the MATLAB/Simulink environment because they needed to study how the system performs when conditions are steady or shifting. It has been observed that the hybrid PV–Wind–SEIG isolated microgrid system combines renewable power supplies and energy storage units with smart management tools so that stability is maintained even though the energy demand fluctuates. This hybrid PV–Wind–SEIG isolated microgrid system contains a Self-Excited Induction Generator (SEIG), a photovoltaic (PV) generation system, a wind energy conversion system, and a Battery Energy Storage System (BESS). The physical arrangement is also made of a DSTATCOM, a bidirectional DC–DC converter, a DTOGI-PLL synchronisation unit, an ANFIS controller, and parts for nonlinear loads.

Energy from the sun is changed into power in the form of electricity while the PV system functions, and the PV system is linked with a DC–DC boost converter which utilizes MPPT control. This MPPT control is used by the system because the highest amount of power must be gathered when irradiance and heat conditions are changing.

Experts claim that the MPPT controller modifies the converter duty ratio at all times so that the PV system remains at the most effective power point. Evidence from the simulation results shows that the MPPT algorithm follows changes in irradiance and nature situations well through the active regulation of the operating voltage and current that belongs to the PV array.

Many researchers claim that the wind energy conversion system is included as an extra natural power source because the wind energy conversion system makes the trustworthiness of the whole system better and increases the power generation strength. Available wind energy is changed into electrical energy by the wind subsystem while active power is given to the isolated microgrid by the wind subsystem. Experts observe that the simulation waveforms show the wind speed quickly reaches a steady working value with very few small variations. This stable performance occurs because the wind energy conversion system makes sure that the energy contribution to the system remains stable.

Self-Excited Induction Generator (SEIG) functions as the primary electricity producing machine for the network that stands alone. Experts claim that capacitor banks are utilized by the system because the Self-Excited Induction Generator (SEIG) needs reactive power support to start its internal field. These groups of capacitors create the needed environment so that the Self-Excited Induction Generator (SEIG) can hold the electrical pressure at its connection points. When the amount of power consumed by the machinery changes, the need for reactive power shifts every moment. This shift creates instability in the electrical pressure and the cycle rate because the Self-Excited Induction Generator (SEIG) faces different pressures from the connected tools. It has been observed that the system is supported by extra help from DSTATCOM and BESS because the Self-Excited Induction Generator (SEIG) must remain steady when the requirement for energy is not constant.

The DSTATCOM is connected at the Point of Common Coupling (PCC) and acts as a power quality improvement device by providing reactive power compensation, harmonic current mitigation and voltage regulation. The DSTATCOM employs a Voltage Source Converter (VSC) connected with a DC-link capacitor and controlled through the proposed ANFIS strategy. During nonlinear load disturbances, the

DSTATCOM injects compensating currents to maintain source current quality and reduce harmonic effects.

The Battery Energy Storage System (BESS) is connected through a bidirectional DC–DC converter to regulate energy flow between the storage system and the DC-link. The BESS performs charging and discharging operations depending upon the active power imbalance between generation and load demand. During transient conditions, the battery supplies or absorbs power to maintain system stability and support frequency regulation.

The synchronisation process of the system is performed using the Dual Second Order Generalised Integrator Phase-Locked Loop (DTOGI-PLL). The DTOGI-PLL extracts accurate phase information even under distorted operating conditions and ensures proper synchronisation between system variables. Performance levels increase because of the synchronisation unit which makes guide signals for the way the controller functions.

Experts say that the ANFIS controller is the main regulating part of the created framework. This controller combines the flexible learning power of artificial neural networks and the logic of fuzzy inference systems so that the best possible regulating signals are produced during different working situations. Instead of using traditional PI controllers, the ANFIS controller changes system factors based on the movement of load needs and the state of the work. It has been observed that faster settling times and better voltage management are reached because of this way of working.

Including nonlinear loads in the system model helps to check how the suggested controller acts during actual working environments. Harmonic currents and quick shifts in electricity requirements are created by the nonlinear load, which brings trouble to the source variables. Waveforms from the simulation show that variation in the nonlinear load started between 2.1 s and 2.3 s, but the resulting transients were fixed by the suggested control approach.

Overall, the MATLAB/Simulink model provides a comprehensive platform for analysing the performance of the proposed hybrid renewable energy system under dynamic operating conditions. The coordinated operation of SEIG, DSTATCOM, BESS, DTOGI-PLL and ANFIS control effectively improves voltage regulation, frequency stability and power quality performance.

4.3 ANFIS Architecture Description

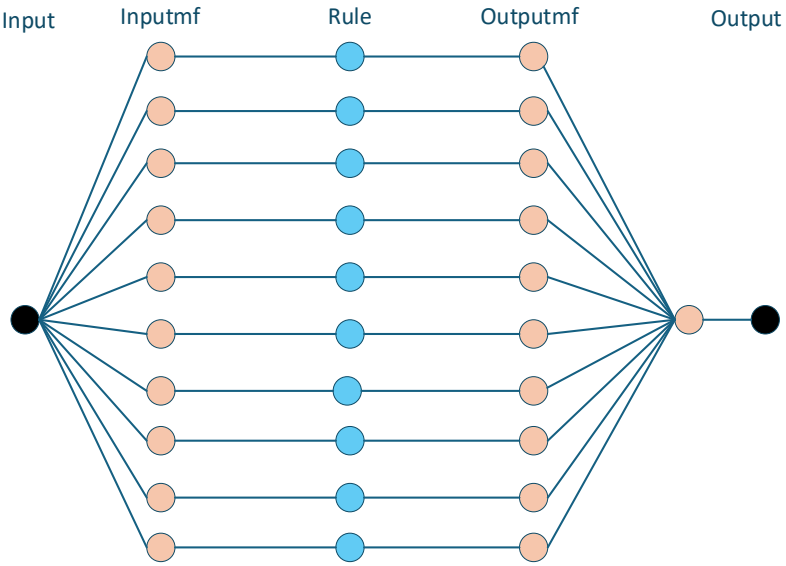

Fig.4.1 Structure of ANFIS

The figure 4.1 illustrates the architecture of the Adaptive Neuro-Fuzzy Inference System (ANFIS), which combines the learning capability of Artificial Neural Networks (ANN) with the reasoning capability of Fuzzy Logic Systems (FLS). ANFIS is designed to establish an intelligent relationship between input variables and output responses by integrating fuzzy decision-making with adaptive learning mechanisms. In the proposed hybrid PV–Wind–SEIG microgrid, ANFIS is employed for frequency regulation and control of dynamic system behaviour under varying operating conditions.

The ANFIS structure shown in the figure consists of five layers, namely the input layer, input membership function layer, rule layer, output membership function layer, and output layer. These layers operate sequentially to process input information and generate an appropriate control signal.

The first layer represents the input layer, where the system input variables are introduced into the ANFIS network. In the proposed controller, these inputs generally correspond to frequency error and change in frequency error. These signals contain information regarding the operating condition of the microgrid and are used for generating corrective control action.

The second layer corresponds to the input membership function layer, where the numerical input values are transformed into fuzzy linguistic variables. This process is

known as fuzzification. The membership function layer determines the degree to which each input belongs to different fuzzy sets such as negative large, negative small, zero, positive small, and positive large. Rather than fixing a single condition to an incoming signal, fuzzy membership permits slow shifts between working zones because fuzzy membership enhances the ability of the guiding system to manage irregular conduct. Experts claim that fuzzy membership provides necessary flexibility for complex data. Gradual transitions are enabled by fuzzy membership so that the guiding system stays stable even though the input changes quickly.

The third layer represents the rule layer, which constitutes the choice-determining part of the ANFIS structure. Every individual point in this section represents a distinct fuzzy rule. Relationships between input requirements and output reactions are established by the rule layer using IF–THEN statements. Because input membership values are joined, the guiding system decides the amount that every rule provides to the whole choice-making path. Many people believe that the rule layer imitates the human thought process when the rule layer picks appropriate management steps according to the state of the apparatus.

The fourth layer is the output membership function layer, where the inputs from every triggered rule are handled and joined together. It has been observed that the output membership function layer identifies the specific weight of every rule for the purpose of creating the final output reaction. Parameters of this section are modified by the adaptive learning capability of ANFIS during the instructional period while the apparatus tries to reach better apparatus functioning and less mistake. Scholars argue that ANFIS relies on these adjustments because the adaptive learning capability of ANFIS needs to reduce deviation constantly.

Within this architecture, the last level serves as the output layer because the separate regulation results are gathered together so one solitary management signal is produced. That solitary management signal functions as the fixing adjustment effort which is needed so that system stability is kept steady. Scientists suggest that the created result is utilized within the suggested microgrid to manage system frequency while the moving reaction is made better.

The intelligent adaptive behaviour is obtained with the complete ANFIS structure, which automatically adapts its system parameters based on the operating data of the system. Unlike conventional controllers, the action of ANFIS changes with varying operating conditions, where the parameters are not fixed a priory. This ability allows for greater accuracy in control and increased robustness in uncertain environments.

The ANFIS architecture has several benefits for renewable energy microgrid applications, includings:

- Improved nonlinear mapping capability
- Better learning and adaptation characteristics
- Faster dynamic response
- Reduced steady-state error
- Enhanced disturbance rejection capability
- Improved frequency regulation performance
- Better stability under varying operating conditions

Thus, the ANFIS architecture shown in the figure provides an effective intelligent control framework for maintaining stable operation and improving the overall performance of the proposed hybrid PV–Wind–SEIG microgrid system.

4.4 Discussion of Results in Steady-State Performance and Dynamic Performance under Load Variation under Nonlinear Loading

87

For the proposed PV–Wind–BESS-based microgrid with DSTATCOM, steady-state and dynamic operating conditions were investigated to enhance the performance of the micro grid using both DTOGI-PLL and ANFIS controller. Robustness and adaptability of the proposed control technique was analysed by adding the nonlinear load variation before the simulation. When observing the acquired waveforms, the disturbance seems to be taking place somewhere in the range of 2.1 s to 2.3 s. The period between this includes transient events caused by a change in current demand. These disturbances cause fluctuations in the demand of active power, reactive power and harmonics which in turn impact the system performance..

Before the load variation ($t < 2.1$ s), the system operates under steady-state conditions where all electrical parameters remain nearly constant and balanced. During this period,

source voltage, source current, load current and converter current maintain stable characteristics with negligible oscillations.

When nonlinear loading is applied during 2.1–2.3 s, disturbances appear in the system due to rapid power demand variation. The DSTATCOM together with BESS and ANFIS controller immediately responds by generating compensating current components to minimise oscillations and maintain stable operation. After transient conditions disappear, the system reaches a new steady-state operating condition.

The obtained simulation results confirm that the proposed control methodology effectively suppresses disturbances, regulates voltage and frequency, improves current quality and enhances power quality performance under nonlinear loading conditions.

4.4.1 Steady-State Performance and Dynamic Behaviour under Load Variation

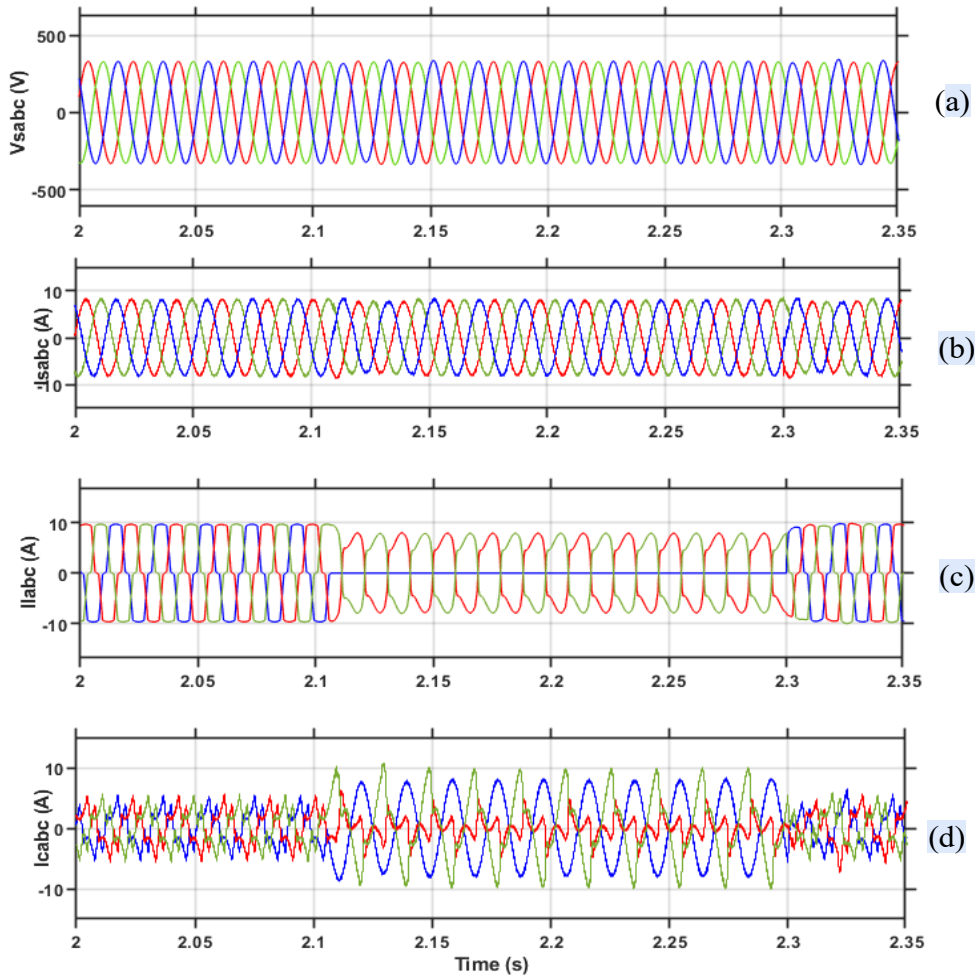

Fig.4.2 Steady-state performance of the proposed DTOGI-PLL–ANFIS control scheme under nonlinear loading. (a)Source Voltage. (b) Source Current. (c)Load Current. (d)Converter Current.

Figure 4.2 illustrates the steady-state and dynamic performance of the proposed ANFIS-based DSTATCOM-controlled hybrid PV–Wind–SEIG microgrid under load

variation conditions. The figure presents the waveforms of source voltage, source current, load current, and converter current. The coordinated operation of the DTOGI-PLL synchronisation technique, ANFIS controller, Battery Energy Storage System (BESS), and DSTATCOM can be clearly observed through these waveforms. The analysis shows the capability of the proposed control strategy to maintain voltage stability, current balancing and dynamic compensation, during changes in load.

Figure 4.1(a) Source Voltage (V_{sabc})

The three-phase source voltage system waveform of the proposed hybrid micro-grid system is shown in the figure 4.1(a). The source voltages may be seen to be well balanced and still close to sinusoidal in nature during operation. Balanced three phases are indicated by the phase voltages being displaced by about 120∘.

The voltage amplitude is essentially unchanged and there is no obvious distortion and not much oscillations. No noticeable voltage sag or swell even during disturbances and load changes in the system. This behaviour will confirm the effectiveness of the coordinated control in providing sufficient voltage regulation operating limits.

The stable voltage profile is attained through a number of orchestrated mechanisms in the system:

- The DSTATCOM continuously provides reactive power support at PCC.
- The Battery Energy Storage System maintains energy balance across the DC-link.
- The DTOGI-PLL accurately tracks system synchronisation signals.
- The ANFIS controller minimises frequency deviations.

The smooth sinusoidal behaviour of the source voltage confirms that the proposed control strategy successfully suppresses disturbances caused by nonlinear loading and renewable power fluctuations. Stable voltage regulation is crucial as the fluctuations in voltage directly impact the power quality and performance of the system.

Moreover, the lack of severe transient oscillations confirms the good damping performances of the controller and the correct coordination between the various control components.

Figure 4.2(b) Source Current (i_{sabc})

Under dynamic operating conditions, the three-phase source current waveform is shown in Figure 4.2(b). It can be noted that the source currents are almost sinusoidal in nature and are in balance.

The waveform exhibits a number of significant features:

- Equal current magnitude among all phases
- Symmetrical current distribution
- Smooth sinusoidal profile
- Reduced current distortion

Although the system experiences variations in load conditions, the source currents continue to maintain stable operation without excessive fluctuations. The proposed controller ensures that the fundamental active power component is supplied from the source and the reactive power and harmonic components are supplied by the DSTATCOM.

This also indicates the successful implementation of the harmonic compensation. From the sinusoidal nature of the source current, it can be inferred that:

- Harmonic components have been effectively removed.
- Reactive current demand is compensated.
- Power factor is improved.
- Current balancing is achieved.

The source current waveform also demonstrates that the proposed ANFIS controller effectively regulates active power flow and maintains system stability during varying operating conditions.

Figure 4.2(c) Load Current (i_{Labc})

The three-phase load current wave form is shown in figure 4.2(c). There is considerable difference in the magnitude of flow when there are variations in load. There is a noticeable change in the characteristics of the load current during the transition period

from the loaddown to the load-up, and it has a "balanced sinusoidal" characteristic during the load down before the change.

The load current variation is dynamic changes in load demand that are connected to the isolated microgrid. In this working window:

- Current magnitude changes considerably
- Phase current characteristics become altered
- Load demand varies rapidly

This behaviour indicates that the connected load imposes varying power requirements on the microgrid system.

A decrease in load current followed by another increase shows a change in the demand for active and/or reactive power. These differences will cause disturbance to a normal isolated system and normally will cause voltage drops and frequency instabilities.

However, even though the load current varies considerably, the source current and source voltage are regulated. This validates that the proposed control system makes the source immune to load disturbances.

The waveform also illustrates that the controller is successful in managing:

- Sudden load changes
- Active power imbalance
- Reactive power variations
- Dynamic system disturbances

Hence, the proposed control approach exhibits strong adaptability under varying load conditions.

Figure 4.2(d) Converter Current (i_{cabc})

The injected converter current is shown in figure 4.2(d). The converter current exhibits highly dynamic behaviour compared with source current and load current because it continuously adjusts itself according to compensation requirements.

It can be observed that the converter current magnitude changes significantly during the load variation interval. This behaviour indicates that the DSTATCOM injects additional compensating current whenever disturbances arise in the system.

The converter current performs several important functions:

- Harmonic current compensation
- Reactive power compensation
- Current balancing
- Voltage support
- Dynamic load compensation

When the load demand changes, the DSTATCOM immediately responds by altering its injected current magnitude and waveform characteristics. During increased compensation requirements, the converter current amplitude increases to supply the required compensating current.

The observed fluctuations in converter current are expected because the DSTATCOM dynamically tracks the required compensation current according to system operating conditions.

The waveform confirms that:

- Converter response is rapid.
- Current tracking accuracy is high.
- Harmonic compensation is effective.
- Dynamic compensation capability is satisfactory.

The rapid variation of converter current demonstrates the effectiveness of the Hysteresis Current Controller and coordinated pulse generation mechanism.

4.4.2 Steady-State Performance of DC-Link Voltage and Frequency Response

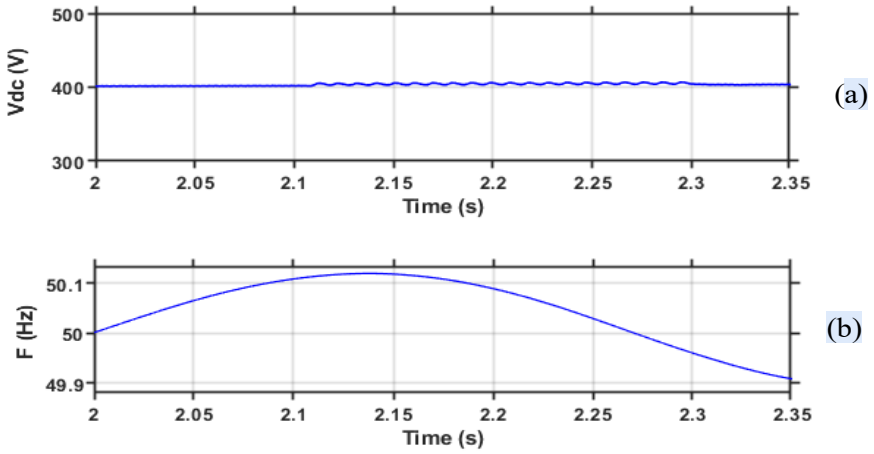

Fig.4.3 Steady-state performance (a)DC Voltage (b)Frequency regulation

Figure 4.3 presents the steady-state and dynamic behaviour of the proposed ANFIS-based hybrid PV–Wind–SEIG microgrid in terms of DC-link voltage and system frequency response. These parameters are highly important because they indicate the effectiveness of the coordinated control strategy in maintaining system stability and ensuring proper operation of the DSTATCOM-interfaced Battery Energy Storage System (BESS). The DC-link voltage reflects the energy balance between the AC and DC sides of the converter, while system frequency indicates the active power balance between generation and load demand. Stable operation of both quantities confirms proper coordination among the ANFIS controller, DTOGI-PLL synchronisation unit, DSTATCOM, and BESS.

Figure 4.3(a) DC-Link Voltage (V_{dc})

Figure 4.3(a) shows the DC-link voltage response of the proposed control system. It can be observed that the DC-link voltage remains approximately around its reference value throughout the operating interval with only very small oscillatory variations.

The waveform indicates a highly regulated and stable DC-link behaviour with negligible fluctuations. Initially, the DC-link voltage reaches its desired operating value and thereafter maintains a nearly constant profile. Minor ripple components can be observed during load transition periods; however, these variations are very small and quickly suppressed by the control system.

The observed behaviour demonstrates the effective operation of the DSTATCOM–BESS coordination strategy because the DC-link voltage is directly associated with energy exchange between the AC side and DC side of the converter. Under varying operating conditions, sudden changes in load demand or renewable generation can create an imbalance between generated and consumed power. Such power mismatch generally causes charging or discharging of the DC-link capacitor and leads to voltage fluctuations.

The stable DC-link voltage response obtained in Figure 4.2(a) indicates that the proposed controller effectively maintains power equilibrium within the system.

Several important observations can be made from the waveform:

- The DC-link voltage remains close to the desired reference value.
- Voltage fluctuations are very small.
- Ripple magnitude is significantly limited.
- No sudden overshoot or undershoot is observed.
- Fast recovery characteristics are achieved.

The small oscillations observed in the waveform are mainly due to:

- Converter switching action
- Dynamic current compensation
- Charging and discharging operation of the battery
- Power fluctuations associated with renewable generation

These oscillations are expected in practical converter systems because the DSTATCOM continuously exchanges energy with the AC network. However, due to the presence of the DC-link capacitor and BESS control mechanism, these disturbances are rapidly attenuated.

The stable DC-link voltage not only verifies the capability of the inverter to deliver a stable voltage to the AC-link, but also rectifies several important properties of the proposed system:

I. **Effective power balancing:**
   By implementing a coordinated battery operation, the generated renewable power and load demand are balanced.

II. **Proper converter operation:**
   A stable DC-link voltage ensures that the Voltage Source Converter can generate appropriate compensating voltages and currents.

III. **Improved transient response:**
   The system quickly restores voltage to its reference value following disturbances.

IV. **Enhanced compensation capability:**
   Maintaining constant DC voltage improves harmonic and reactive power compensation.

Hence, the resulting waveform shows that the proposed coordinated control strategy can successfully control the DC-link voltage and ensure the stability of the converter.

Figure 4.3(b) System Frequency Response (*F*)

The system frequency response of the proposed hybrid micro-grid is shown in figure 4.3(b), with different operating conditions. The frequency waveform is in very close proximity to the nominal operating frequency with slight deviations around the reference frequency.

It is seen that the frequency first rises a little, then falls steadily to the nominal operating level. The frequency variation is very small in the operating range and doesn't show any oscillatory instability.

This behaviour demonstrates the effectiveness of the ANFIS controller in maintaining frequency stability under dynamic operating conditions.

In isolated microgrids, frequency is highly sensitive to active power imbalance because no utility grid exists to provide support. Whenever generated power becomes greater than load demand, the system frequency tends to increase. Conversely, when load demand exceeds generated power, frequency decreases.

The very small frequency variation observed in the figure indicates that the proposed control system effectively compensates for power imbalance and maintains stable system operation.

The frequency regulation performance can be attributed to several coordinated actions within the proposed control strategy:

I. **ANFIS-based adaptive control:**
   The ANFIS controller continuously processes frequency deviation and generates suitable corrective action according to system operating conditions.

II. **Battery Energy Storage System support:**
   The battery absorbs or supplies active power whenever renewable generation fluctuates.

III. **DTOGI-PLL synchronisation:**
   Accurate estimation of phase angle and frequency improves overall control precision.

IV. **DSTATCOM operation:**
   The converter assists in maintaining system stability through coordinated current compensation.

Several important observations can be drawn from the frequency response:

- Frequency remains very close to nominal value.
- Oscillations are extremely small.
- Dynamic response is smooth.
- No abrupt variations are present.
- Fast recovery capability is achieved.

The absence of severe frequency oscillations indicates that the proposed controller successfully suppresses disturbances associated with renewable power variations and load changes.

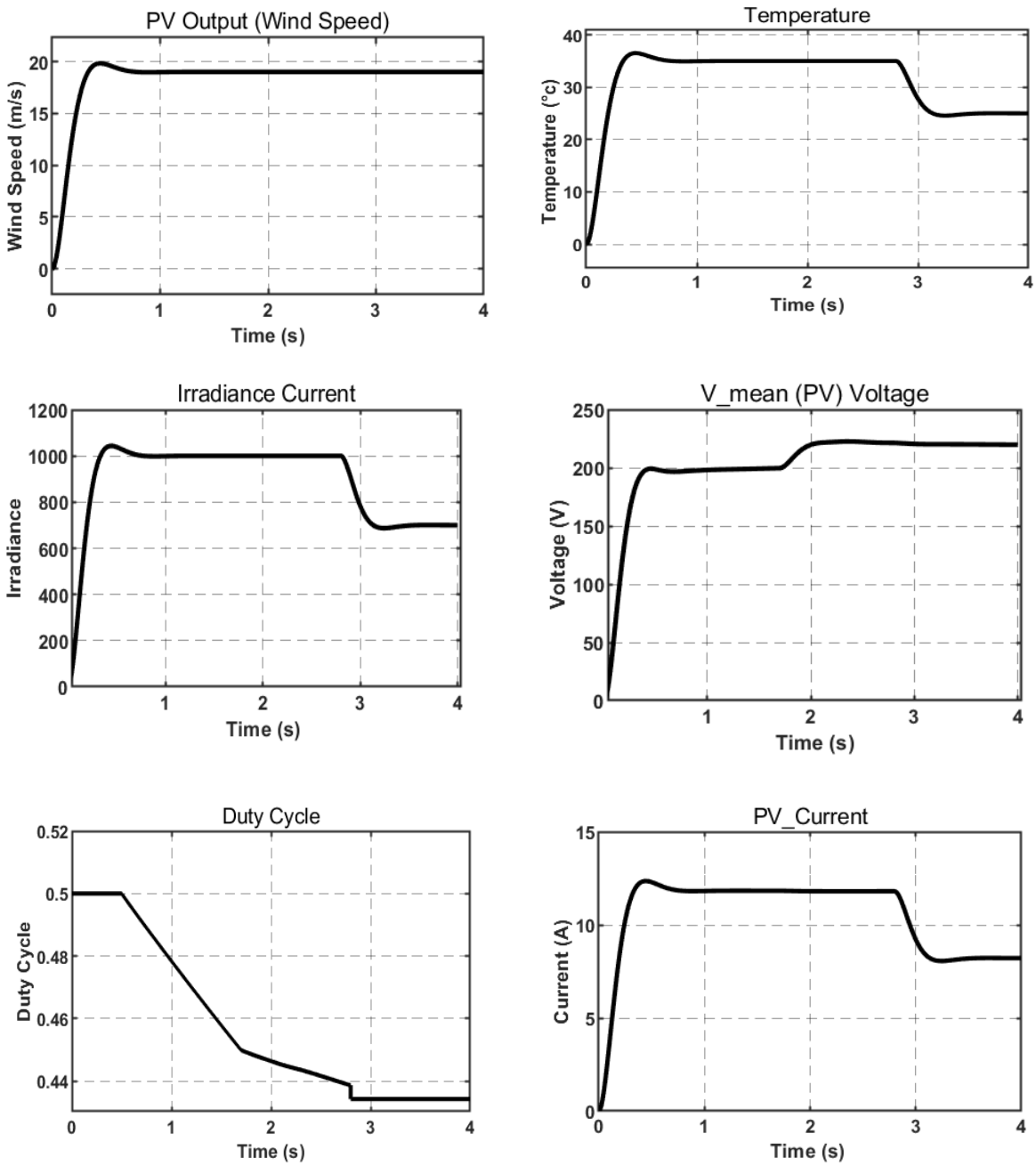

Fig.4.4 PV–MPPT simulation results. (a)Wind Speed. (b)Temperature. (c)Irradiance Current (d)PV voltage (e)Duty Cycle (f)PV Current

Figure 4.4 illustrates the dynamic performance of the Solar Photovoltaic (SPV) generation system under changing environmental conditions. The figure presents the variations in wind speed input, temperature, solar irradiance, PV voltage, duty cycle, and PV current response. The obtained waveforms demonstrate the effectiveness of the Maximum Power Point Tracking (MPPT) control strategy in maintaining stable photovoltaic operation under varying atmospheric conditions. Since the output characteristics of a photovoltaic system are highly nonlinear and strongly dependent

upon environmental parameters, evaluation of these characteristics becomes essential for analysing the dynamic behaviour of the overall hybrid PV–Wind–SEIG microgrid.

96 The results show that the proposed MPPT controller continuously adjusts the operating point of the photovoltaic system according to changes in environmental conditions and ensures efficient power extraction.

Figure 4.3(a) Wind Speed Input Characteristics

Figure 4.3(a) illustrates the variation of wind speed considered during system operation. Initially, the wind speed is rapidly rising and becomes almost steady for the wind power after a short transient period. There is a small transient (overshoot) at the start followed by a steady state value.

The waveform exhibits smooth characteristics and lacks sudden changes or oscillations. The steady increase and leveling off of wind speed show the steady variations of wind power available in the real environment and hence the hybrid renewable system performs under realistic operating conditions.

The following observations can be made from the waveform:

- Wind speed reaches stable operating conditions rapidly.
- Overshoot magnitude remains very small.
- No continuous oscillatory behaviour is observed.
- Stable environmental input conditions are maintained.

The stable wind profile contributes to maintaining a consistent power contribution from the wind generation system and supports overall system reliability.

Figure 4.3(b) Temperature Characteristics

The variation in the PV cell temperature under dynamic operating conditions is presented in Figure 4.3(b). The temperature starts to rise quickly to a higher operating point, then drops back down to a new stable operating point.

The observed temperature behavior shows the variation in the atmosphere that the PV system experiences during operation. As the PV's output characteristics is very

temperature-dependent, changes in temperature will directly impact the electrical parameters of the PV array.

The PV system is affected by the temperature variation as follows:

- PV voltage decreases with rising temperatures.
- The efficiency of power generation is impacted by an increase in temperature.
- The operating point of the PV Array varies with temperature change.
- Maximum power output is affected by changes in cell temperature.

The waveform shows continuous transitions without abrupt changes, suggesting consistent environmental changes.

Important observations include:

- Temperature changes occur gradually.
- System response remains stable.
- No large oscillatory behaviour is observed.
- Environmental variations are effectively accommodated.

Figure 4.3(c) Solar Irradiance Characteristics

Figure 4.3(c) presents the variation in solar irradiance supplied to the photovoltaic array. The irradiance will initially rise sharply, and then become high. Then, a decrease in the irradiance can be seen, which is related to changes in sunlight intensity.

The amount of energy that strikes the surface of the PV array is directly proportional to solar irradiance, and thus has a significant influence on power generation capability.

The waveform shows several features:

- High irradiance produces increased photovoltaic output power.
- Reduction in irradiance decreases generated current magnitude.
- Environmental changes alter photovoltaic operating conditions.
- Smooth dynamic transitions between the operating regions are made.

The observed decrease in irradiance could be an actual situation in the environment, including:

- Cloud movement
- Weather changes
- Partial shading effects
- Variations in solar intensity

The absence of abrupt fluctuations confirms stable system operation under changing environmental conditions.

Figure 4.3(d) Mean PV Voltage Characteristics

The mean output voltage of the PV array is shown in Figure 4.3(d). The first part of the waveform is steeply rising and the second part is at a predetermined operating point. Voltage magnitude variation is seen in the voltage when operating conditions change and then it is almost steady.

The voltage behaviour shows that the operating point of the PV array is consequently switched by the MPPT controller when the environment changes.

The observed waveform is showing:

- Rapid voltage rise during initial operation.
- Small overshoot during transition.
- Stable operating behaviour after settling.
- Smooth voltage regulation characteristics.

The stable voltage response confirms effective operation of the MPPT control mechanism because the controller continuously modifies converter operation to maintain the photovoltaic system near its maximum power operating point.

Moreover, the voltage is not severely oscillating, implying the good dynamic response, and hence, better tracking performance.

Figure 4.3(e) Duty Cycle Characteristics

The duty cycle response of the DC–DC converter which operates the MPPT control strategy is illustrated in Figure 4.3(e). The duty cycle is continuously varying as related to the variability in the operating conditions of photovoltaic elements.

Initially, the duty ratio is higher and gradually reduces as controller varies the operating point of the PV system.

The reason behind the variation of duty cycle is due to the adaptive operation of the MPPT controller:

- The operation of the converter changes based on the changes in irradiance.
- The PV voltage is not constant, therefore the duty cycle needs to be adjusted accordingly.
- The controller brings the operating point into the maximum power area.

The gradual change in duty cycle indicates:

- Smooth converter operation
- Stable MPPT tracking
- Reduced oscillation around operating point
- Improved dynamic response

The absence of rapid fluctuations confirms that the controller does not produce unstable switching behaviour.

Figure 4.3(f) PV Current Characteristics

Figure 4.3(f) shows the output current of the PV array. The waveform starts very fast, then levels off to almost a steady value. Later, reduction is noted in the magnitude of the current in accordance with the changes in irradiance.

The photovoltaic cu is directly proportional to incident solar radiation, so changes in PV irradiance will directly impact the output current.

From the waveform, it can be observed that it has the following properties:

- Increase in irradiance increases PV current.
- Reduction in irradiance decreases output current.
- Operates under variable conditions in a stable fashion.
- Dynamic response remains smooth.

The decrease in the current after irradiance change proves the proper behavior of the PV system and demonstrates the effectiveness of the MPPT control method.

4.4.3 Harmonic Analysis of Source Current Using FFT

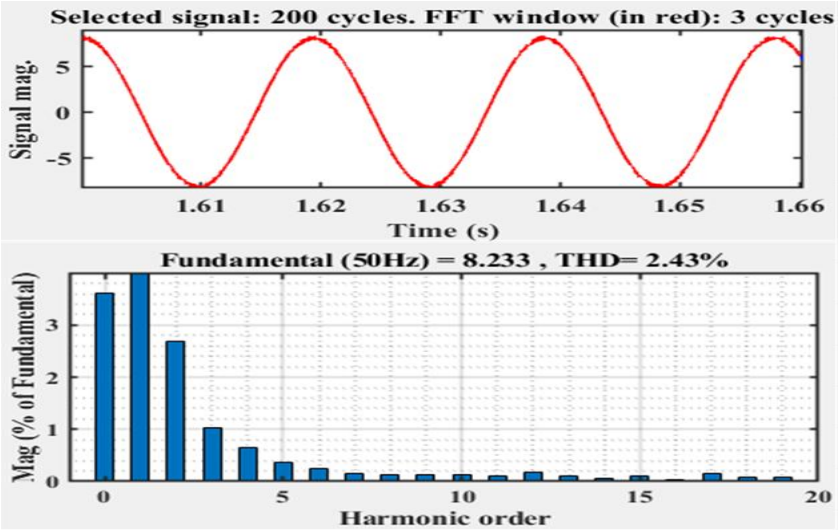

Fig.4.5 THD of Source Current

The Fast Fourier Transform (FFT) analysis of the source current waveform from the proposed microgrid configuration, which is an ANFIS controlled hybrid PV–Wind–SEIG microgrid system, is shown in Fig. 4.5. The FFT analysis is carried out to check the presence of the harmonic content in the measured current and to verify the reduction of the total harmonic distortion by the proposed control method. The main reasons for the harmonic analysis to be used as an important performance indicator is to identify the extent to which electrical power supplied by the system is of good quality and to ensure that it conforms to power quality standards.

The upper portion of the plot shows the section of the source current waveform that was selected for harmonic analysis. The waveform is smooth and is almost sinusoidal in appearance with uniform positive and negative half cycles. The current characteristics observed are clear signs of a balanced system in operation, as well as compensation of the undesirable current components. It can be seen that the proposed DSTATCOM-interfaced control strategy is effective in eliminating harmonics generated by nonlinear loads without noticeable waveform distortion.

The harmonic spectrum of the source current (FFT) is displayed in the lower part of the figure. The harmonic spectrum shows the relative amount of each individual harmonic frequency, compared to the fundamental frequency of the current signal. The level of each harmonic is shown in a percentage of the fundamental current.

From the results of the FFT it can be seen that the fundamental component has the largest magnitude, and the higher order harmonics have considerably reduced amplitudes. In the third, fifth and seventh harmonics, the distortion of the current is normally significant in nonlinear systems. But these harmonic components are greatly reduced in the obtained results because of the working of the proposed control strategy.

There are some conclusions that may be reached from the harmonic spectrum:

- The fundamental current component dominates the overall current waveform.
- Higher-order harmonic magnitudes remain extremely small.
- Harmonic amplitudes decrease rapidly with increasing harmonic order.
- No dominant harmonic component is observed.
- Current waveform remains close to an ideal sinusoidal signal.

The Total Harmonic Distortion (THD) value obtained from the FFT analysis is approximately **2.43%**, which indicates a very low level of current distortion within the system. The simulation results of the obtained THD level verify the effectiveness of suppressing the harmonic components and the good quality of the power performance afforded by the proposed coordinated control strategy.

The combined effect of a few control components is responsible for this lower THD value:

I. **DTOGI-PLL synchronisation technique:**
   The DTOGI-PLL correctly identifies the fundamental positive sequence component of distorted current signals and suppresses the harmonic disturbances.

II. **ANFIS controller:**
   The ANFIS controller adaptively regulates system variables and improves current tracking performance under changing operating conditions.

III. **DSTATCOM operation:**
The DSTATCOM injects compensating currents to eliminate harmonic and reactive current components from the source side.

IV. **Hysteresis Current Controller:**
The hysteresis controller generates accurate switching pulses and enables rapid current tracking capability.

V. **Battery Energy Storage System support:**
The BESS assists in maintaining DC-link voltage stability and improves dynamic compensation capability.

According to power quality standards, particularly IEEE harmonic recommendations, the current harmonic distortion should remain within acceptable limits to ensure reliable system operation and prevent undesirable effects such as excessive heating, increased power losses, equipment malfunction, and reduced efficiency. The obtained THD value satisfies the permissible harmonic limits and demonstrates that the proposed microgrid system operates within acceptable power quality requirements.

The reduced harmonic distortion also provides several operational advantages, including:

- Improved power factor
- Reduced converter and transmission losses
- Lower heating effects in electrical equipment
- Enhanced system efficiency
- Improved reliability of connected loads
- Better dynamic performance

Therefore, the FFT analysis presented in Figure 4.4 confirms the effectiveness of the proposed ANFIS-based DSTATCOM control strategy in suppressing harmonic components and maintaining high-quality power within the isolated hybrid PV–Wind–SEIG microgrid system. The results are obtained, and the capability of the proposed system to provide better power quality and meet the harmonics performance limits is validated with the obtained results under different operating conditions.

4.4.5 Comparative Dynamic Performance Analysis of Proposed DTOGI–ANFIS and Conventional SRF–PLL Control Technique

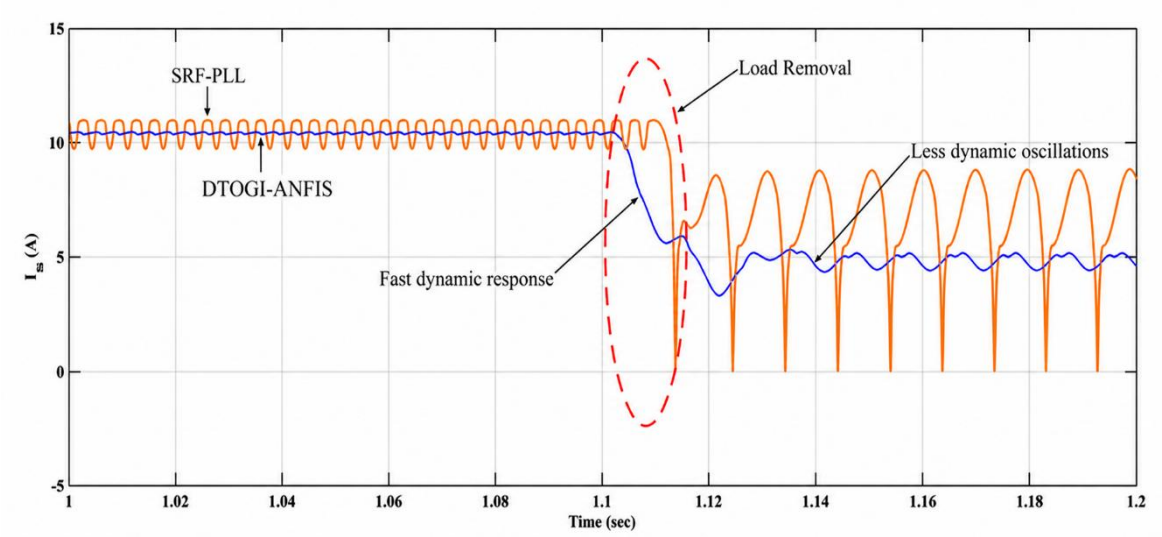

Fig.4.6 Performance Comparison of the Proposed DTOGI-PLL and Conventional SRF-PLL Controllers Under Load Variation Conditions.

The comparative performance analysis for the proposed DTOGI–ANFIS control technique with the conventional SRF–PLL based control method is shown in Figure 4.6 under dynamic load variation conditions. The figure shows the source current response of both the control options employed during a load removal disturbance condition. Comparative analysis is conducted to study the dynamic behaviour, transient response, oscillation behaviour and rejection capability of the proposed controller.

As any disturbance affecting the system will influence the current behaviour, the source current response is an important indicator that is used to evaluate the controller. When there are sudden load changes, the active power becomes out of balance in isolated renewable energy systems, potentially causing transient oscillations, current distortion, and instability. So, a controller which has faster dynamic response with better disturbance rejection property needs to be used to get stable system operation.

The current response can be divided into two parts as seen in Figure 4.5:

- **Orange waveform:** Conventional SRF–PLL-based control technique
- **Blue waveform:** Proposed DTOGI–ANFIS control technique

The results indicate a significant difference in the dynamic behaviour of the two approaches.

I. Performance of Conventional SRF–PLL Control Technique

The source current spectrum for the SRF–PLL control method shows noticeable oscillatory behaviour over the entire operating range. Before the occurrence of the disturbance condition, the current waveform contains continuous oscillations around the operating point.

The conventional SRF–PLL method shows the following characteristics:

- Presence of continuous dynamic oscillations
- Larger current fluctuations
- Slow transient response
- Higher settling behaviour
- Increased sensitivity to disturbances

During the load removal condition, a significant variation in source current magnitude is observed. The current response undergoes large fluctuations and exhibits repeated oscillatory behaviour before approaching its steady operating condition.

The larger oscillations can be attributed to the inherent limitations of SRF–PLL under distorted operating conditions. Since SRF–PLL directly relies on synchronous reference frame transformation, it becomes sensitive to:

- Harmonic distortion
- System nonlinearities
- Frequency variations
- Transient disturbances

Consequently, the controller produces delayed compensation action and exhibits poor disturbance rejection capability.

Furthermore, the repeated oscillatory behaviour indicates that the controller requires a longer duration to restore stable operating conditions after a disturbance occurs.

II. Performance of Proposed DTOGI–ANFIS Control Technique

105 The blue waveform in Figure 4.5 represents the source current response of the proposed DTOGI–ANFIS control strategy. Compared with the conventional method, the proposed controller demonstrates significantly improved dynamic behaviour.

The operating point is nearly stable, and the current has very small oscillatory variations about the operating point initially. The waveform has a smoother shape and stable operating characteristics.

During load removal, a transient change in current magnitude is seen, and the controller quickly counters this, bringing current back to its desired operating condition.

The proposed controller response displays several important characteristics:

- Faster disturbance rejection capability
- Reduced current oscillations
- Smooth transient response
- Improved stability characteristics
- Lower steady-state fluctuation
- Rapid current recovery

The improved performance is primarily due to the combined operation of DTOGI synchronisation and ANFIS-based adaptive control.

The DTOGI synchronisation algorithm offers:

- Accurate extraction of fundamental positive sequence components
- Better harmonic suppression capability
- Effective elimination of DC-offset components
- Improved phase estimation accuracy

Simultaneously, the ANFIS controller offers adaptive learning features through continuous adjustment of control parameters under the different operating conditions of the system.

Due to this adaptive mechanism:

- The controller quickly detects system disturbances.
- Corrective action is generated rapidly.
- Current deviation is minimised.
- Stable operation is restored efficiently.

III. Dynamic Behaviour during Load Removal Condition

The highlighted region in Figure 4.5 is the system response for load removal conditions. The removal of load causes a sudden drop in active power demand and thus causes power imbalances in the isolated microgrid.

Under such conditions:

- Source current decreases rapidly
- Frequency tends to increase
- Transient disturbances are introduced
- Dynamic compensation becomes necessary

The proposed DTOGI–ANFIS controller responds rapidly and minimises transient effects. In contrast, the conventional SRF–PLL shows larger fluctuations and slow stabilisation behaviour.

The proposed control system provides for:

I. Fast dynamic response:

The controller automatically senses the varied conditions in the system and produces corrective action.

II. Reduced dynamic oscillations:

Current oscillations are significantly minimised after disturbance occurrence.

III. Improved stability:

The present waveform is smoothly approaching its steady operating condition.

IV. Better disturbance rejection:

The controller effectively suppresses transient disturbances.

V. Comparative Observations from Figure 4.5

Based on the comparative analysis, the following observations can be made:

- The proposed DTOGI–ANFIS method exhibits faster dynamic response.
- Dynamic oscillations are significantly reduced.
- The SRF–PLL method exhibits larger fluctuations.
- The proposed controller achieves smoother current characteristics.
- Disturbance rejection capability is improved.
- Stability under varying operating conditions is enhanced.
- Current tracking performance is superior

CHAPTER 5

CONCLUSION

5.1 Overview of the Proposed Research Work

In the current research work, focus has been given to designing and modelling a hybrid PV–Wind–SEIG based isolated microgrid with a DSTATCOM interfaced Battery Energy Storage System (BESS) for enhancing the power quality and ensuring stable operation of the microgrid system. The proposed system utilized the renewable energy sources for sustainable power generation and addressed the operational challenges of isolated microgrid environments. Unlike with grid support, voltage stability, frequency control, and power quality in isolated systems are critical concerns when operating under different conditions.

In order to overcome these problems, a coordinated control approach that includes DTOGIPLL synchronisation and ANFIS frequency control was designed and applied in MATLAB/Simulink. The controller proposed was used to control the dynamics of the system under conditions of changes in load and under nonlinear operating conditions. The system's ability to support reactive power load, its harmonic compensation capability and the ability to balance energy were further enhanced by the integration of DSTATCOM and BESS.

5.2 Performance of Proposed Control Methodology

The simulation results showed that the proposed control approach was capable of keeping the hybrid renewable energy system's operation stable under different operating conditions. ANFIS controller, DTOGI–PLL synchronisation technique, DSTATCOM and BESS achieved adequate current compensation and improved the dynamic performance of the system.

The ANFIS controller exhibited good adaptability to the system frequency by continually adjusting the system's control action to meet the varying system conditions. The results showed that the proposed method had less oscillatory behaviour, better disturbance rejection and better dynamic response than the conventional control

methods. The outcomes further showed good coordination of active and reactive power control during transient operating conditions.

5.3 Power Quality Improvement and Harmonic Mitigation

The main goal of the research was to enhance power quality performance in the case of nonlinear loading conditions. It was found that the DSTATCOM-based compensation scheme resulted in a reduction in the level of harmonic distortion, and the source currents were balanced. Even with changing load, the source current waveforms were found to be almost sinusoidal with good operation of the harmonic compensation mechanism.

54

The Total Harmonic Distortion value was found to be within the acceptable limits as per the IEEE standards using Fast Fourier Transform analysis. The decreased harmonic content confirmed the ability of the proposed controller to reduce the undesirable harmonic components produced by nonlinear loads. Power losses, power factor and overall system efficiency were also improved due to improved harmonic mitigation.

5.4 Voltage and Frequency Regulation Performance

The simulation results showed good voltage and frequency regulation performance under various operating conditions. The operating voltage of the source was balanced and kept its amplitude almost constant during the operating time. Likewise, the frequency response showed small deviations around the nominal operating point which showed the effective active power balancing capability.

Working together, Battery Energy Storage System and DSTATCOM were important to help maintain stability of the DC-link voltage and meet transient power demands when working together. The BESS helped mitigate power imbalance by charging up or discharging the electricity grid in response to the instability of renewable electricity generation, increasing system stability. The proposed control strategy was thought to enable the continuous operation of the isolated microgrid under dynamics.

5.5 Overall Conclusions and Future Scope

Overall, the results of this research confirm the effectiveness of the proposed coordinated control strategy to enhance the performance of an isolated hybrid PV–Wind–SEIG microgrid. The developed system with different operating modes regulates the voltage, stabilises the frequency, mitigates the harmonics and compensates for the dynamic load while keeping the system stable. The proposed DTOGI–ANFIS control technique was also found to be better than the traditional synchronisation techniques in terms of dynamic oscillations reduction and transient behaviour improvement.

The results obtained are very satisfactory, but there are still opportunities for future improvement. Advanced intelligent optimisation techniques can be used to automatically tune the controller parameters. Furthermore, the system can be further optimized in terms of practical implementation and performance by implementing machine learning-based predictive control algorithms, real-time hardware validation on the DSP or FPGA platform, and adding more renewable energy sources. These advancements can help with the reliability, flexibility and efficiency of future off-grid renewable energy systems.

REFERENCES

[1] J. M. Guerrero, J. C. Vasquez, J. Matas, L. G. de Vicuña, and M. Castilla, "Hierarchical control of droop-controlled AC and DC microgrids—A general approach toward standardization," IEEE Trans. Ind. Electron., vol. 58, no. 1, pp. 158–172, Jan. 2011, doi: 10.1109/TIE.2010.2066534.

[2] E. Levi, "Self-excited induction generators for renewable energy applications," *IEE Proc.-Electr. Power Appl.*, vol. 143, no. 6, pp. 481–490, Nov. 1996, doi: 10.1049/ip-epa:19960442..

[3] S. S. Murthy, O. P. Malik, and A. K. Tandon, "Analysis of self-excited induction generators," *IEEE Trans. Energy Convers.*, vol. 3, no. 2, pp. 254–260, Jun. 1988, doi: 10.1109/60.4442.

[4] J. M. Elder, J. T. Boys, and J. L. Woodward, "Self-excited induction machine as a small low-cost generator," *IEE Proc. C*, vol. 131, no. 2, pp. 33–41, Mar. 1984, doi: 10.1049/ip-c.1984.0006.

[5] R. C. Bansal, "Three-phase self-excited induction generators: An overview," *IEEE Trans. Energy Convers.*, vol. 20, no. 2, pp. 292–299, Jun. 2005, doi: 10.1109/TEC.2004.847955.

[6] F. Blaabjerg, R. Teodorescu, M. Liserre, and A. V. Timbus, "Overview of control and grid synchronization for distributed power generation systems," *IEEE Trans. Ind. Electron.*, vol. 53, no. 5, pp. 1398–1409, Oct. 2006, doi: 10.1109/TIE.2006.881997.

[7] S. Golestan, J. M. Guerrero, and J. C. Vasquez, "Single-phase PLLs: A review of recent advances," *IEEE Trans. Power Electron.*, vol. 34, no. 4, pp. 3130–3143, Apr. 2019, doi: 10.1109/TPEL.2018.2844254.

[8] M. Ciobotaru, R. Teodorescu, and F. Blaabjerg, "A new single-phase PLL structure based on second-order generalized integrator," in *Proc. IEEE PESC*, 2006, pp. 1–6, doi: 10.1109/PESC.2006.1711988.

[9] M. Karimi-Ghartemani and M. R. Iravani, "A method for synchronization of power electronic converters in polluted and variable-frequency environments," *IEEE Trans. Power Syst.*, vol. 19, no. 3, pp. 1263–1270, Aug. 2004, doi: 10.1109/TPWRS.2004.831279.

[10] P. Rodríguez, A. Luna, I. Candela, R. Mujal, R. Teodorescu, and F. Blaabjerg, "Multiresonant frequency-locked loop for grid synchronization of power converters under distorted grid conditions," *IEEE Trans. Ind. Electron.*, vol. 58, no. 1, pp. 127–138, Jan. 2011, doi: 10.1109/TIE.2010.2042420.

[11] B. Singh, S. Murthy, and S. Gupta, "Analysis and design of STATCOM-based voltage regulator for self-excited induction generators," IEEE Trans. Energy Convers., vol. 19, no. 4, pp. 783–790, Dec. 2004, doi: 10.1109/TEC.2004.827707.

[12] S. Golestan, J. M. Guerrero, and J. C. Vasquez, "Three-phase PLLs: A review of recent advances," *IEEE Trans. Power Electron.*, vol. 32, no. 3, pp. 1894–1907, Mar. 2017, doi: 10.1109/TPEL.2016.2574303.

[13] B. Singh, A. Chandra, and K. Al-Haddad, "Power quality: Problems and mitigation techniques," *Wiley*, 2015, doi: 10.1002/9781118922064.

[14] J. S. R. Jang, "ANFIS: Adaptive-network-based fuzzy inference system," *IEEE Trans. Syst., Man, Cybern.*, vol. 23, no. 3, pp. 665–685, May–Jun. 1993, doi: 10.1109/21.256541.

[15] M. H. Rashid, *Power Electronics Handbook*, 4th ed., Butterworth-Heinemann, 2018.

[16] A. Jain and B. Singh, "A voltage and frequency control scheme for standalone wind energy conversion system," *IET Renew. Power Gener.*, vol. 10, no. 6, pp. 774–783, 2016, doi: 10.1049/iet-rpg.2015.0377.

[17] H. Akagi, E. H. Watanabe, and M. Aredes, *Instantaneous Power Theory and Applications to Power Conditioning*, Wiley, 2017, doi: 10.1002/9781119307181.

[18] S. Roy, A. Das, and P. Sensarma, "Control of grid-integrated DFIG–SPV–BESS-based hybrid microgrid system," *IEEE Trans. Ind. Appl.*, vol. 60, no. 2, pp. 1450–1462, Mar.–Apr. 2024, doi: 10.1109/TIA.2023.3321456.

[19] P. Sinha, S. Bajpai, A. Arora, P. Chittora and D. Shailly, "DTOGI-CDSC-FLL based synchronization and control of WEC-PV-BESS-based distributed generation system," 2025 7th International Conference on Energy, Power and Environment (ICEPE), Shillong, India, 2025, pp. 1-6

[20] A. Mahela, O. P. Mahela, and A. G. Shaik, "Power quality improvement in renewable energy sources based power system using DSTATCOM supported by battery energy storage system," in Proc. IEEE Int. Conf. Power, Instrum. Control Comput. (PICC), Thrissur, India, 2018, pp. 1–6, doi: 10.1109/PICC.2018.8719318.